IDŐJÁRÁS

QUARTERLY JOURNAL
OF THE HUNGARIAN METEOROLOGICAL SERVICE

CONTENTS

****

http://www.met.hu/firat/ido-e.html

VOL. 101 * NO. 4 * OCTOBER–DECEMBER 1997

IDŐJÁRÁS

Quarterly Journal of the Hungarian Meteorological Service

Editorial Office: P.O. Box 39, H-1675 Budapest, Hungary or
Gilice tér 39, H-1181 Budapest, Hungary
E-mail: gmajor@met.hu or *antal@met.hu*
Fax: (36-1) 290-7387

Subscription by

mail: IDŐJÁRÁS, P.O. Box 39, H-1675 Budapest, Hungary;
E-mail: gmajor@met.hu or *antal@met.hu*; *Fax: (36-1) 290-7387*

IDŐJÁRÁS
Quarterly Journal of the Hungarian Meteorological Service
Vol. 101, No. 4, October–December 1997, pp. 239–260

Application of two methods for N_2O emission estimates to Bulgaria and the Netherlands

Carolien Kroeze[1] and **Stanislav Bogdanov**[2]

[1]*Wageningen Institute for Environment and Climate Research*
Wageningen Agricultural University,
P.O. Box 9101, 6700 HB Wageningen, The Netherlands;
E-mail: carolien.kroeze@wimek.cmkw.wau.nl

[2]*National Institute of Meteorology and Hydrology*
66 Tsarigradsko chaussee 1784, Sofia, Bulgaria
E-mail: stas@ozon.rthsf.meteo.bg

(Manuscript received 2 January 1997; final form 14 July 1997)

Abstract—Nitrous oxide (N_2O) is one of the greenhouse gases in the earth's atmosphere. This study focuses on two methodologies for estimating N_2O emissions at the national scale: a method developed in the Netherlands (NEO method), and the IPCC Guidelines for National Greenhouse Gas Inventories (IPCC method). The purpose of this study is: (i) to apply both the IPCC and NEO methods to Bulgaria and the Netherlands, (ii) to investigate differences between the NEO and IPCC methods and (iii) to compare emissions from Bulgaria to emissions from the Netherlands.

There are a number of differences between the NEO and IPCC methods. First, the NEO method includes more sources of N_2O than the IPCC method. Second, some emissions are estimated in different ways. Due to these differences the IPCC method results in higher total emissions than the NEO method: for both countries IPCC emissions are about 20% higher than those of the NEO method (mid-point estimates). These differences result from a net effect; for some sources the IPCC method exceeds the NEO method (in particular for agriculture) and for others the IPCC estimates are lower. The sources not included in the IPCC method are natural emissions, enhanced background emissions from mineral soils, N_2O induced by NO_x deposition, chemical industries other than nitric and adipic acid production, atmospheric formation of N_2O, use in anaesthesia, enhanced emissions due to global warming and aquatic emissions due to non-agricultural nitrogen inputs.

NEO and IPCC estimates for N_2O emissions from Bulgaria are 24 and 29 Gg N y^{-1}, respectively, and from the Netherlands 37 and 45 Gg N y^{-1} (mid-point estimates). Thus annual anthropogenic N_2O emissions from the Netherlands are about 15 Gg N_2O-N higher than those from Bulgaria. Dutch emissions exceed Bulgarian in particular for the following sources: agriculture, traffic and nitric acid production. These differences are caused by differences in human activities mainly.

Key-words: nitrous oxide, N_2O, Bulgaria, The Netherlands, greenhouse gas inventory.

1. Introduction

Nitrous oxide (N_2O) is one of the gases contributing to the enhanced greenhouse effect (*Houghton et al.,* 1995). The atmospheric concentrations of N_2O have been increasing (*Prinn et al.,* 1990), because of human activities. Food production, energy use, industry and production of waste result in emissions of N_2O. Worldwide emissions are nowadays 50% higher than in pre-industrial times (*Bouwman et al.,* 1995). Agriculture is one of the most important sources of N_2O. Global inventories indicate that about two-thirds of the anthropogenic nitrous oxide emissions are related to human food production (e.g. *Bouwman et al.,* 1995; *Nevison et al.,* 1996).

Bulgaria and the Netherlands, like all other parties to the United Nations Framework Convention on Climate Change (UNFCCC), agreed to report their national greenhouse gas emissions. Most countries estimate their N_2O emissions following the IPCC Guidelines for National Greenhouse Gas Inventories (*IPCC/OECD,* 1995, 1997). These guidelines provide default methodologies for estimating greenhouse gas emissions on a national scale. Although IPCC Guidelines are available, countries are free to use their own, country-specific methods. For Bulgaria an inventory of N_2O emissions exists, which was made following the 1995 IPCC Guidelines for Greenhouse Gas Inventories, using default emission factors (*Bogdanov,* 1995, 1996).

The Netherlands is one of the few countries that reported N_2O emissions using an alternative method (*Van Amstel et al.,* 1994; *VROM,* 1994). The Dutch method is based on a review of experimental studies in and outside the Netherlands (referenced in *Kroeze,* 1994, 1995). Other than in the Netherlands, no experimental studies on N_2O emissions have been performed for Bulgaria. This implies that a Bulgarian inventory should be based on data from other regions of the world. In the present study we will investigate to what extent the Dutch method, or NEO method, is applicable to Bulgaria and to what extent it differs from the IPCC Guidelines (IPCC method). This would not only result in an improved insight into Bulgarian emissions, but it would also contribute to the evaluation of inventory methods in general. The purpose of this study is: (i) to apply both the IPCC and NEO methods to Bulgaria and the Netherlands, (ii) to investigate differences between the NEO and IPCC methods and (iii) to compare emissions from Bulgaria to emissions from the Netherlands.

2. Methods for estimating national N_2O emissions

In this study two methods for estimating N_2O emissions are compared: the IPCC Guidelines for national Greenhouse Gas Inventories (*IPCC/OECD,* 1995, 1997) and a Dutch methodology developed for the Dutch National Environmental Outlooks (NEO) by the National Institute for Public Health and Environmental Protection (*Kroeze,* 1994, 1995).

3. IPCC Guidelines for National Greenhouse Gas Inventories (IPCC method; Box 1)

The IPCC method was developed such that it is applicable to any country of the world. It should assist countries in reporting their emissions as required for parties to the United Framework Convention on Climate Change. In the IPCC method emissions are estimated by applying a given (default) emission factor to activity data. The input data needed are usually available from existing databases such as those provided by the Food and Agricultural Organization (FAO). The following sources of N_2O are considered in the IPCC Guidelines: agriculture, waste, energy, and industry (*IPCC/OECD,* 1995, 1997). The most important sources are described below (see also *Box 1*).

In 1995 the first version of the IPCC Guidelines was published (*IPCC/-OECD,* 1995). An evaluation resulted in Phase II Guidelines (*IPCC/OECD,* 1997), which differs from the existing guidelines for N_2O emissions from agriculture and waste (sewage) (*Mosier et al.,* in press). In the present study we will use this updated version of the IPCC Guidelines.

3.1 Agriculture

Agriculture is one of the most important sources of N_2O and gives rise to short-term and long-term emissions of N_2O. The updated (Phase II) IPCC method aims at considering the full nitrogen cycle. Three sources of N_2O related to the N cycle are distinguished in the IPCC method (*Mosier et al.,* in press):

- (i) direct emissions from agricultural soils, taking place as a result of fertilization of soils,
- (ii) emissions from animal production and
- (iii) N_2O produced after the nitrogen leaves the agricultural field (indirect emissions).

The direct emissions from agricultural fields take place shortly after nitrogen additions to soils (*Mosier,* 1994). In the IPCC Guidelines direct emissions are estimated as 1.25 (0.25–2.25)% of the nitrogen input from fertilizers, biological nitrogen fixation or crop residues, in line with the work by *Bouwman* (1996). The N input is from synthetic and organic fertilizers, nitrogen in crop residues and from nitrogen fixing plants. Another source of direct soil emissions of N_2O are cultivated histosols. These are assumed to emit 5 kg N_2O-N per hectare in regions with temperate or boreal climates and 10 kg N_2O-N per hectare in the tropics.

Animals are the second agricultural sources of N_2O considered in the IPCC Guidelines (*Oenema,* 1995). Animals not only cause N_2O emissions when manure is used as fertilizer, but also when manure is stored in stables or during grazing of animals (e.g. *Bouwman et al.,* 1995; *Velthof* and *Oenema*, 1994a).

Box 1. Summary of IPCC method for estimating N_2O emissions (kg N y^{-1}); see for a detailed description *IPCC/OECD* (1995, 1997) and *Mosier et al.* (in press)

Agriculture

direct soil emissions = EF1 · N-INPUT + EF2 · AREAHIS
animal related emissions = sum ($EF3_t$ · $N\text{-}AWMS_t$)
indirect emissions = EF4 · (NO_x + NH_3) + EF5 · NLEACH

Waste

emissions from waste incineration = EF6 · MSW
emissions from sewage treatment = EF7 · NSEWAGE

Energy

emissions from stationary combustion = EF8 · FUEL
emission from mobile combustion = EF9 · KM

Industry

emissions from adipic acid production = EF10 · AA
emissions from nitric acid production = EF11 · NA, where

EF1	= 0.0125 (0.0025–0.0225) kg N_2O-N/kg N/y
EF2	= 5 or 10 kg N_2O-N per hectare of histosol per year
EF3	= emission factor in kg N_2O-N/kg N/y = 0.001 (<0.002) for anaerobic lagoon and liquid systems; 0.02 (0.005–0.03) for solid storage, dry lot, pasture range and paddock; 0.005 for other systems
EF4	= 0.01 (0.002–0.02) kg N_2O-N/kg N/y
EF5	= 0.025 (0.002–0.12) kg N_2O-N/kg N/y
EF6	= 0.019 (0.006–0.127) kg N_2O-N/kg MSW incinerated
EF7	= 0.01 (0.002–0.12) kg N_2O-N/kg N/y
EF8	= 0.064 (0–0.7), 0.382 (0–1.782) and 0.891 (0–6.343) g N_2O-N/GJ, for gas, oil and coal, respectively
EF9	= emission factors for several types of vehicles (see *IPCC/OECD*, 1995)
EF10	= 0.191 kg N_2O-N/kg adipic acid
EF11	= 17 (7–27) g N_2O-N/kg nitric acid
N-INPUT	= N input to soils from fertilizers (excluding NH_3 emissions), crop residue and N fixation (kg N y^{-1}) = Fsn + Faw + Fbn + Fcr
Fsn	= synthetic fertilizer use (kg N y^{-1}) excluding 10% that is emitted as NH_3 and NO_x
Faw	= manure N used as fertilizer = manure N produced · (1 – (fraction produced in meadows + fraction lost as NH_3 + fraction used for fuel)); manure production in meadows is from *IPCC/-OECD* (1997), 20% of manure-N is lost as NH_3 and 0% used as fuel in Bulgaria and the Netherlands
Fbn	= biological N fixation (kg N y^{-1}) = 3% of the dry matter legume production = 3% of twice the production of pulses and soybean as reported by FAO
Fcr	= N in crop residues left on the field (kg N y^{-1}); calculated as 55% of the total N in crop biomass (assuming 45% is removed as crop) = 45% of 3% and 1.6% of the dry matter production of legumes and other crops, respectively = 45% of 3% and 1.6% of twice the production of pulses/soybean and other crops in FAO data, respectively
AREAHIS	= area of cultivated histosols in the country (ha)
N-AWMS	= manure N produced in different types (t) of Animal Waste Management Systems (AWMS) (kg N y^{-1}) estimated from default values for N excretion per animal and fraction of N produced per type of AWMS from *IPCC/OECD* (1997)
NO_x + NH3	= NO_x and NH_3 emitted in the country (kg N y^{-1})
NLEACH	= N leaching (kg N y^{-1}) = 30% of N-INPUT
NSEWAGE	= human sewage N production (kg N y^{-1}) = 16% of annual protein intake in kg
MSW	= municipal solid waste incineration (kg y^{-1})
FUEL	= stationary combustion of gas, coal and oil (GJ y^{-1})
KM	= vehicle-kilometers (km y^{-1}) or fuel use (GJ y^{-1}) per vehicle type
NA	= nitric acid production (kg y^{-1})
AA	= adipic acid production (kg y^{-1})
t	= type of AWMS

The related N_2O emissions are estimated as a percentage of the amount of nitrogen produced by animals in different animal waste management systems (Box 1). The starting point for the calculations is the nitrogen excretion by different six animal types (dairy cattle, non-dairy cattle, poultry, sheep, swine and other) in six different animal waste managing systems, AWMSs (anaerobic lagoon, liquid systems, solid storage and dry lot, pasture range and paddock, and other systems). The phase II method of IPCC provides default values for emission factors (% of manure-N that is lost as N_2O for different AWMSs), manure-N production per animal type (kg N animal^{-1} y^{-1}) and the percentage of manure-N that is produced in different AWMSs (% per animal type) for eight regions, among which there are Eastern Europe (including Bulgaria) and Western Europe (including the Netherlands). These default factors for nitrogen excretion in different waste management systems are based on *Ecetoc* (1994), *Safley et al.* (1992), *Vetter et al.* (1989) and *Steffens* and *Vetter* (1990) mainly. The N_2O emission factors are based on a review of experimental studies, listed in *IPCC/OECD* (1997). The only input data needed to calculate N_2O emissions in the IPCC method are animal numbers in the country.

The third agricultural source of N_2O includes the indirect emissions. Indirect emissions of N_2O take place when nitrogen leaves the agricultural fields as gas (ammonia or nitrogen oxides) or as leached nitrogen and is converted to N_2O by bacteria in remote soils or in aquatic systems. The IPCC method estimates indirect emissions as a result of NH_3 or NO_x losses as 1% of the amount of NH_3-N and NO_x-N emitted (Box 1). This is within the range of direct emissions from agricultural soils, and in line with findings by *Bowden et al.* (1991) and *Brumme* and *Beese* (1992). The amount of N from manure and fertilizers that leaches is assumed to be 30% of the total manure and fertilizer nitrogen applied. After leaching, this nitrogen may be nitrified or denitrified, giving rise to emissions of N_2O from rivers and estuaries (*Seitzinger,* 1988, 1990). The emission factor for indirect emissions due to leaching is 2.5% (Box 1), and deduced from extensive literature review (*IPCC/OECD,* 1997).

3.2 Waste

In the IPCC Guidelines two sources of N_2O are included that are related to waste handling: (i) incineration of municipal solid waste (MSW) and (ii) sewage treatment. MSW incineration gives rise to abiogenic N_2O formation (Box 1). Emissions from sewage take place in sewage treatment plants or when the sewage is discharged on surface waters. In the IPCC method the N flux in human sewage is determined on the basis of annual intake of proteins in which the fraction of N is 0.16 (*IPCC/OECD,* 1997). The daily intake per capita in the world varies between 55 and 110 g protein day^{-1}. The related N_2O emissions are calculated as 1% of the amount of N in the sewage (Box 1).

3.3 Energy

The IPCC method provides default emission factors for the stationary combustion of gas, coal and oil (Box 1). However, an emission factor for fluidized bed combustors (FBC) in utility boilers is not provided, while these systems are known to emit more N_2O than conventional coal-fired power plants. In addition, the IPCC method provides emission factors for traffic (listed in *IPCC/OECD,* 1995, 1997).

3.4 Industry

The IPCC method considers process N_2O emissions during production of nitric and adipic acid (*IPCC/OECD,* 1995, 1997). In both Bulgaria and the Netherlands nitric acid is produced, but no adipic acid. The activity data needed are the amounts of HNO_3 produced.

4. Method developed for Netherlands Environmental Outlook (NEO method; Box 2)

The NEO method includes N_2O of both anthropogenic (i.e. resulting from human activities) and natural (i.e. not induced by human activities) origin:

$$\textit{total emissions} = \textit{anthropogenic} + \textit{natural emissions}.$$

In addition, the NEO method distinguishes between biogenic (i.e. of biological origin) and abiogenic emissions. The biogenic emissions are estimated as:

$$\textit{biogenic emissions} = EFb \cdot \textit{N-INPUT} + \textit{background},$$

where *EFb* is an emission factor for biogenic emissions, *N-INPUT* is the anthropogenic nitrogen flux to, for instance, soils and waters (kg N y^{-1}), and *background* is the natural plus enhanced background emissions. *EFb* is based on a review of available data, including studies performed in the Netherlands (EF12 and EF14 in *Box 2*). Background emissions may be enhanced due to, for instance, lowering of the ground water level. The total background emissions are calculated as 10 (1–20) and 1 (0.5–5) kg N ha^{-1} y^{-1} for organic and mineral soils, respectively, and the values are mainly based on *Velthof* and *Oenema* (1994b) and *Bouwman* (1996). The natural part of this is, for the Netherlands, estimated from model simulations by *Bouwman* and *van der Hoek* (1991).

Abiogenic emissions are estimated as:

$$\textit{abiogenic emission} = EFa \cdot \textit{ACTIVITY} + \textit{abiogenic natural source},$$

Box 2. Summary of NEO method for estimating N_2O emissions (kg N y^{-1}); see for a detailed description *Kroeze* (1994, 1995)

Natural

natural biogenic N_2O = natural background emissions from soils[1]
natural abiogenic N_2O = atmospheric formation = 0.1% of NH_3-N emission[2]

Agriculture

biogenic N_2O from soils and leached N = EF12 · N-INPUT + background emissions[1]

Waste

emissions from waste incineration = EF13 · MSW
emissions from sewage treatment = EF14 · NSEWAGE

Energy

emissions from stationary combustion = EF15 · FUEL
emission from mobile combustion = EF16 · KM

Industry

emissions from adipic acid production = as IPCC method (Box 1)
emissions from nitric acid production = as IPCC method (Box 1)
other chemical industry = in-country estimate

Other

atmospheric formation = 0.1% of NH_3-N emission[2]
N_2O due to non-agricultural N inputs to surface waters = N-INPUT · EF12
atmospheric deposition of non-agricultural NH3 = NH3 emission · EF12
atmospheric deposition of non-agricultural NO_x = NO_x emission · EF12
emissions from anaesthesia = use in anaesthesia

where

EF12	= emission factor (kg N_2O-N per kg N) = 0.1 (0.002–0.125), except for anaerobic storage of manure when EF12 = <0.002; N-inputs to organic soils, manure injected to soils, urine patches and biological treatment of manure when EF12 = 0.2 (0.125–0.25); and nitric acid added to manure and aerobic storage of manure, when EF12 = 0.5 (0.25–0.1)
EF13	= 12.7 (3.2–127) g N_2O-N per ton of MSW (from *Spoelstra* (1993) and IPCC method)
EF14	= 0.1 (0.002–0.125) kg N_2O-N per kg N removal in sewage treatment
EF15	= same as IPCC method (Box 1) except for fluidized bed combustion (FBC) when EF15 = 26.7 (4.4–49) G N_2O-N GJ^{-1} (from *Spoelstra*, 1993)
EF16	= emission factors for several types of vehicles (from *Baas*, 1991)
N-INPUT	= Nitrogen flux (kg N y^{-1}): synthetic fertilizer, animal manure, atmospheric deposition of NH_3 or NOx, biological N_2 fixation, nitrogen leaching, sewage

MSW, NSEWAGE, FUEL, KM: see Box 1

---

[1] from *Velthof* and *Oenema* (1994a), *Bouwman* (1996) and *Bouwman* and *van der Hoek* (1991)
[2] *Dentener* (personal communication)

where *EFa* is an emission factor for abiogenic emissions, *ACTIVITY* is the human activity considered, and *abiogenic natural source* include N_2O formation in the unpolluted atmosphere mainly. *EFa* is partly based on IPCC emission factors, and partly on *Baas* (1991, 1994), *Spoelstra* (1993) and *Dentener* (personal communication) (EF13, EF15 and EF16 in Box 2). A detailed description of the NEO method is referred in *Kroeze* (1994, 1995). In the following a description is given of the most important differences between the IPCC and NEO methods.

4.1 Natural emissions

Natural sources include soils, waters and the atmosphere. In soils, bacteria produce N_2O during nitrification and denitrification. These natural background emissions are estimated for the Netherlands by use of model calculations (*Bouwman* and *van der Hoek*, 1991). Natural emissions from aquatic sources could not be quantified. In the atmosphere, N_2O is formed during the oxidation of NH_3. The NEO method assumes that 0.1% of NH_3 emitted is oxidized to N_2O in the Netherlands, of which 10% is natural and 90% is anthropogenic (*Dentener,* personal communication).

4.2 Agriculture

The most important differences between the NEO and IPCC methods for agriculture are caused by differences in emission factors used (Box 1 and 2). For instance, the direct emissions from agricultural soils depend on the type of soil in the NEO method. The NEO emission factors used are 1 (0.2–1.25)% of the N applied for mineral soil and 2 (1.25–2.5)% for organic soil. In the IPCC method differences in soil type are not considered.

Second, emission factors for animal manure in stables differ. The IPCC method is more detailed in this respect (Box 1). In the NEO method only three types of manure storage are considered: anaerobic storage with low emissions, aerobic storage with relatively high emissions, and the manure to which nitric acid has been added in order to avoid emissions of NH_3. Nitric acid addition is nowadays not a common practice in the Netherlands.

Another difference between the two methods is the presumed evaporation of NH_3 from fertilizers and manure (in the NEO method it is mostly based on *Van der Hoek,* 1994). For instance, NEO method assumes that 2% of synthetic fertilizers volatilize as NH_3, as opposed to 10% in the IPCC method. This can be explained by the fact that in the Netherlands virtually no fertilizers are used that give rise to NH_3 emissions (e.g. urea and anhydrous ammonia). The NEO method further assumes that about 8% of the manure N produced in meadows evaporates as NH_3. Of the remaining manure-N about 60% is urine and 40% is faeces, to which N_2O emission factors of 2 and 1% are applied, respectively (Box 2). Assumptions about NH_3 emissions from stables also differ: the NEO method assumes that about 15% of manure N in stables is emitted as NH_3.

Nitrous oxide emissions related to leaching are calculated differently in the two methods. The NEO method assumes that 20% of the manure and fertilizers applied to soils leaches to the ground water (as opposed to 30% in the IPCC method) and the applied NEO emission factor is 1% (as opposed to 2.5% in the IPCC method). In addition, the methods use different default factors for N excretion by livestock.

Finally, the number of sources included in the two methods differ. The NEO method includes background emissions from both organic and mineral soils. The IPCC method, however, only includes background emissions from cultivated organic soils (histosols). Alternatively, the IPCC method considers crop residues that are left on the field as external N input (Box 1), while the NEO method does not.

4.3 Waste

For municipal solid waste (MSW) incineration the NEO method adopts an emission factor based on measurements in Dutch waste incineration (*Spoelstra,* 1993). This emission factor is 10% lower than the IPCC emission factor. The emission from sewage in NEO is estimated according to the quantity of N removed from the sewage and the nitrogen in the influent and the effluent of the waste water treatment. The applied emission factor is 1%.

4.4 Energy and industry

NEO emissions related to energy use and industrial processes are for most processes estimated as in the IPCC method. Exceptions are fluidized bed combustion and traffic, for which the NEO method uses emission factors that were derived from Dutch studies (*Spoelstra,* 1993; *Baas,* 1991, 1994). In addition, the NEO method includes chemical industries other than adipic and nitric acid production.

5. Nitrous oxide emissions from Bulgaria: IPCC and NEO methods

The emissions of N_2O presented for Bulgaria refer to 1988, since this year was chosen as base year for Bulgaria under the United Nations Frame Convention on Climate Change (UNFCCC). The emissions as calculated following the IPCC method are presented in *Tables 1* and *2* and are from *Bogdanov* (1995, 1996) with the exception of emissions from agriculture and sewage (this study).

Table 1. Nitrogen and nitrous oxide fluxes in Bulgarian and Dutch agriculture (IPCC method[1]) in Gg N y^{-1} (ranges are based on ranges in emission factors)

	Bulgaria		The Netherlands	
	Activity	N_2O emission	Activity	N_2O emission
Direct soil emissions				
Direct soil emissions	N input[2]		N input[2]	
- synthetic fertilizer	385	4.8 (1.0–8.7)	370	4.6 (0.9–8.3)
- animal waste	136	1.7 (0.3–3.1)	521	6.5 (1.3–11.7)
- biological N fixation	11	0.1 (0.0–0.3)	5	0.1 (0.0–0.1)
- crop residue	92	1.2 (0.2–2.1)	25	0.3 (0.1–0.6)
Histosols	Area (ha)		Area (ha)	
- area (ha)	0	0.0 (0.0 - 0.0)	274124	1.4 (0.6–4.1)
Animal production				
	N production			
anaerobic lagoon	4	0.0 (0.0–0.0)	0	0.0 (0.0–0.0)
liquid	59	0.1 (0.0–0.1)	420	0.4 (0.0–0.8)
daily spread	0	0.0 (0.0–0.0)	62	0.0 (0.0–0.0)
solid/dry lot	56	1.1 (0.3–1.7)	122	2.4 (0.6–3.7)
pasture/paddock	151	3.0 (0.8–4.5)	103	2.1 (0.5–3.1)
other	95	0.5 (0.5–0.5)	71	0.4 (0.4–0.4)
Indirect N_2O emission				
	N flux			
NH_3 deposition	116	1.2 (0.2–2.3)	196	2.0 (0.4–3.9)
leaching	238	6.0 (0.5–28.6)	355	8.9 (0.7–42.6)
Total		19.6 (3.8–51.7)		29.0 (5.4–79.3)

[1] see Box 1; input data for Bulgaria are from *FAO* (1990) and for the Netherlands from *Kroeze* (1994, 1995)

[2] Fsn + Faw + Fbn + Fcr (see Box 1)

Table 2. IPCC method: N_2O emissions from Bulgaria and the Netherlands in Gg N_2O-N y^{-1} (ranges are based on ranges in emission factors)

	Bulgaria[1]	**The Netherlands**[2]
Agriculture		
direct soil emissions	7.8 (1.6–14.0)	12.9 (2.9–24.9)
animal emissions	4.7 (1.5–6.8)	5.3 (1.5–7.9)
indirect emissions	7.1 (0.7–30.9)	10.8 (1.1–46.5)
Total	19.6 (3.8–51.7)	29.0 (5.4–79.3)
Waste		
MSW incineration	0.0 (0.0–0.0)	0.1 (0.0–0.4)
sewage	0.6 (0.1–6.9)	0.8 (0.2–9.6)
Total	0.6 (0.1–6.9)	0.9 (0.2–10.0)
Energy		
stationary combustion	3.5 (0.5–26.8)	0.6 (0.0–4.4)
mobile combustion	0.2 (0.1–0.4)	3.7 (1.0–6.3)
Total	3.7 (0.6–27.2)	4.3 (1.0–10.7)
Industry		
nitric acid production	4.9 (2.0–7.8)	10.5 (4.3–16.7)
adipic acid production	0.0 (0.0–0.0)	0.0 (0.0–0.0)
Total	4.9 (2.0–7.8)	10.5 (4.3–16.7)
Total anthropogenic N_2O	28.8 (6.5–93.7)	44.7 (10.9–116.8)

[1] *Bogdanov* (1995), except emissions from agriculture and sewage (this study); ranges are based on ranges in emission factors;
[2] *Kroeze* (1994, 1995), except emissions from agriculture and sewage (this study); ranges are based on ranges in emission factors

Total emissions from Bulgaria calculated using the IPCC method amount to 29 (7–94) Gg N_2O-N y^{-1}. Agriculture is the most important contributor to these emissions, contributing by about two-thirds to total emissions. The input data needed for the IPCC method (Box 1), including fertilizer use, animal numbers and crop production are from *FAO* (1990). In Bulgaria 428 Gg of fertilizer N was used in 1988, mostly as ammonium nitrate (thus Fsn = 385 Gg N). The livestock in the country produced 365 Gg N from which 41% (151 Gg N) was deposited in meadows during pasture and 59% in stables. About 170 Gg of manure-N was used as fertilizer (in-country estimate; thus Faw = 136 Gg N). There are no histosols in Bulgaria, and the area of arable land and permanent crops amounts to 4.1 million hectare (grasslands are not fertilized). Production of pulses and soybeans amounts to 177 Gg, giving rise to 11 Gg of nitrogen added to soils (Fbn). Similarly, 92 Gg of N is input to soils from crop residues (Fcr), as calculated from FAO crop production data and following Box 1. For estimating the emission of N_2O from human sewage following the IPCC method, the annual nitrogen flux in human nutrition is needed as input. In Bulgaria, daily protein intake amounts to 110 g protein^{-1} person^{-1} day (*FAO*, 1990), giving rise to 0.6 (0.1–6.9) Gg N_2O-N emitted annually.

The NEO method estimates Bulgarian emissions at 24 (8–52) Gg N_2O-N. These emissions are found to be largely anthropogenic (*Tables 3* and *4*). The application of the NEO method to Bulgaria required a few additional assumptions, in particular with respect to background emissions from soils. Background emissions are partly natural, and partly a result of agricultural practices (Box 2). For the Netherlands the natural part of the background emissions has been estimated based on country-specific model results, while total current background emissions were estimated from measurements in Dutch soils. For Bulgaria such calculations and measurements have not been performed, so that additional assumptions were needed. For the Netherlands the default emission factor for total background emissions is 10 (1–20) kg N_2O-N ha^{-1} y^{-1} for grassland on organic soil and 1 (0.5–5) kg N_2O-N ha^{-1} y^{-1} for grassland and arable land on mineral soil. Since in Bulgaria there are no organic soils, it is reasonable to assume for Bulgaria that the emission factor for background emissions amounts to 1 kg N_2O-N ha^{-1} y^{-1}, half of which may be natural.

Energy and industry related emissions account for about one-third of Bulgarian emissions according to the NEO method (Table 3) and are calculated from fuel use, car mileage and nitric acid production as presented in *Bogdanov* (1995, 1996). The difference between the IPCC and NEO estimates for Bulgarian traffic emissions is a result of different emission factors used (Box 1 and 2).

Almost two-thirds of Bulgarian emissions are from agriculture according to the NEO method (Tables 3 and 4). The input data on fertilizer use, animal numbers and land area are from FAO (*FAO,* 1990). Animal manure production is calculated by use of the default factors for nitrogen excretion from the IPCC method. And ammonia emissions are estimated using the emission factors provided by the NEO method: 2 and 20% of synthetic and organic fertilizer use, respectively, and 8% and 15% of manure-N produced in meadows and stables, respectively. In the NEO method nitrogen leaching is estimated as 20% of the N input to soils.

Table 3. Agricultural emissions from Bulgaria (NEO method) in Gg N_2O–N y^{-1} (ranges are based on ranges in emission factors)

	Activity level (Gg N)[1]	N_2O emission (Gg Ny^{-1})[2]
Background	4100000 hectare	2.1 (1.0–10.3)
Synthetic fertilizer (excluding NH_3)		
- on mineral soil	419	4.2 (0.8–5.2)
- on organic soil	0	0.0 (0.0–0.0)
Animal manure (excluding NH_3)		
Produced in meadows		
- urine (60%)	83	1.7 (1.0–2.1)
- faeces (40%)	56	0.6 (0.1 – 0.7)
Produced in stables		
- aerobic storage	47	2.4 (1.2–4.7)
- anaerobic storage	133	0.1 (0.0–0.3)
Applied to soils		
- mineral soils	115	1.2 (0.2–1.4)
- organic soils	0	0.0 (0.0–0.0)
- injection	0	0.0 (0.0–0.0)
NH_3 emissions		
manure	74	0.7 (0.2–0.9)
synthetic fertilizer	9	0.1 (0.0–0.1)
Biological N fixation	11	0.1 (0.0–0.1)
Leaching	113	1.1 (0.2–1.4)
Total		14.2 (4.8–27.3)

[1] except when mentioned otherwise;
[2] ranges are based on ranges in emission factors

Table 4. NEO method: N_2O emissions from Bulgaria and the Netherlands in Gg N y^{-1} (ranges are based on ranges in emission factors); n.q. = not quantified

	Bulgaria[1]	**The Netherlands**[2]
Natural emissions		
soils	2.1 (1.0–10.3)	1.5 (0.5–3.0)
atmospheric form.	0.0 (0.0–0.0)	0.0 (0.0–0.0)
Total	2.1 (1.0–10.3)	1.5 (0.5–3.0)
Anthropogenic emissions		
Agriculture		
background	2.1 (1.0–10.3)	3.0 (0.6–11.1)
fertilizer	4.2 (0.8–5.2)	4.4 (1.2–5.5)
manure meadows	2.2 (1.2–2.8)	2.2 (1.1–2.7)
manure stables	2.5 (1.2–5.0)	0.5 (0.1–0.9)
manure fertilizer	1.2 (0.2–1.4)	3.2 (1.0–4.0)
NH_3 emission	0.8 (0.2–1.0)	1.6 (0.3–2.1)
legumes	0.1 (0.0–0.1)	0.2 (0.0–0.2)
leaching	1.1 (0.2–1.4)	1.8 (0.4–2.3)
Total	14.2 (4.8–27.3)	16.9 (4.7–28.8)
Waste		
MSW incineration	0.0 (0.0–0.0)	0.0 (0.0–0.4)
sewage	0.1 (0.0–0.2)	0.3 (0.1–0.3)
Total	0.1 (0.0–0.2)	0.3 (0.1–0.8)
Energy		
stationary combustion	0.5 (0.0–3.5)	0.7 (0.0–4.5)
mobile combustion	0.3 (0.1–1.0)	3.4 (1.5–11.5)
NO_x emission	1.6 (0.3–2.1)	1.2 (0.2–1.5)
Total	2.5 (0.4–6.5)	5.4 (1.8–17.5)
Industry		
nitric acid	4.9 (2.0–7.8)	10.5 (4.3–16.7)
adipic acid	0.0 (0.0–0.0)	0.0 (0.0–0.0)
other	0.0 (0.0–0.0)	1.1 (1.1–1.1)
Total	4.9 (2.0–7.8)	11.6 (5.4–17.7)
Other		
atmospheric formation	0.0 (0.0–0.0)	0.0 (0.0–0.1)
other N-loading	n.q.	0.6 (0.1–0.7)
other NH_3 emission	0.0 (0.0–0.0)	0.1 (0.0–0.2)
other NO_x emission	0.0 (0.0–0.0)	0.5 (0.1–0.6)
anaesthesia	0.0 (0.0–0.0)	0.3 (0.3–0.3)
Total	0.0 (0.0–0.0)	1.6 (0.6–1.9)
Total anthropogenic	21.7 (7.3–41.8)	35.6 (12.5–66.7)
Total N_2O	23.7 (8.3–52.1)	37.1 (13.0–69.7)

[1] this study; [2] *Kroeze* (1994, 1995)

Waste and the category "other" are moderate sources of N_2O in Bulgaria in the NEO estimate (Table 4). It is assumed here that there is no municipal solid waste (MSW) incineration. The NEO method calculates emissions from sewage treatment plants based on the amount of N removed during treatment of municipal waste water. In Bulgaria, however, data on N removal are scarce and waste water treatment may not be as commonly applied as in the Netherlands. Tentatively assuming equal per capita N removal rates in Bulgaria and the Netherlands, N removal in Bulgaria is estimated at 15.5 Gg N y^{-1}. The related N_2O emissions in Bulgaria are estimated here as 0.1 (0.0–0.2) Gg N y^{-1}. Emissions of N_2O due to non-agricultural N-loading to waters have not been quantified due to the lack of input data.

6. Nitrous oxide emissions from the Netherlands: IPCC and NEO methods

Dutch nitrous oxide emissions in 1990 according to the NEO and IPCC methods have been published in *Kroeze* (1994, 1995), with the exception of agricultural and sewage-related emissions following the IPCC Phase II method (Table 1). Total emissions are 45 (11–117) Gg N_2O-N y^{-1} for the IPCC method and 37 (13–70) Gg N_2O-N y^{-1} for the NEO method (Tables 2 and 4).

The emissions from agriculture are 29 (5–79) Gg N_2O-N y^{-1} according to the revised IPCC method (Table 1). This is based on estimates for total nitrogen input to Dutch soils (N-INPUT in Box 1) amounting to 922 Gg N y^{-1} from synthetic fertilizers (excluding ammonia emissions), animal waste (excluding ammonia emissions), biological N fixation and crop residues. The total use of synthetic fertilizer in the Netherlands is 412 Gg N y^{-1} (*RIVM,* 1993) and according to the IPCC methodology 10% of this is lost as NH_3 (so that Fsn = 370 Gg N; Table 1). Animal manure production amounts to 780 Gg N y^{-1}, of which 20% is lost as NH_3 according to the IPCC method and 13% is produced in meadows (thus Faw = 521 Gg N; Table 1). The nitrogen input from N-fixing crops (Fbn) is calculated as 6% of the dry biomass production of pulses and soybean. In the Netherlands dry pulses production amounts to 83 Gg y^{-1} (*FAO,* 1990); the related N input is therefore 5 Gg N y^{-1} (Table 1). Nitrogen in crop residue (Fcr) is, in the IPCC methodology, estimated as 55% of the total N in crop, where total N in crop is 6% of dry pulses and soybean produced and 3% of dry production of other crops (i.e. 1352 Gg of cereals in the Netherlands (*FAO,* 1990)). Nitrogen input from crop residue in the Netherlands would therefore be 25 Gg N y^{-1} (Table 1). Finally, the area of organic soil in the Netherlands is 274124 hectare (*Van Amstel et al.,* 1994). Other input data used for the Netherlands are presented in detail in *Kroeze* (1994, 1995). This present (phase II) IPCC estimate for agricultural emissions (29 Gg N) is much higher than the 2.4 Gg N as estimated following the previous (phase I) IPCC Guidelines as a result of more sources included and higher emission factors used (*Kroeze*, 1995).

7. N_2O emissions: IPCC method versus NEO method

The N_2O emissions for both Bulgaria and the Netherlands are summarized in *Figs. 1, 2* and *3*. The IPCC Phase II method results in total N_2O emissions that are about 20% higher than the NEO estimate for Bulgaria and the Netherlands, respectively. These differences in mid-point estimates result from a net effect; for some sources the IPCC method exceeds the NEO method (agriculture, waste and, for Bulgaria, energy) while for others the IPCC estimates are lower than or equal to the NEO estimates (natural emissions, industry, other and, for the Netherlands, energy). The difference between the two methods is larger for Bulgaria than for the Netherlands, because of the difference in N_2O estimates from stationary combustion mainly.

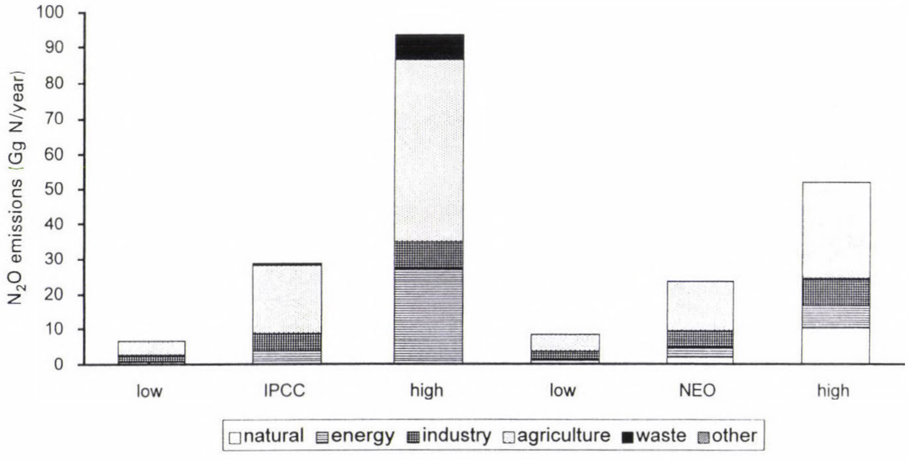

Fig. 1. Bulgarian 1988 emissions of N_2O estimated following the IPCC and NEO methods. Low and high estimates refer to ranges in emission factors (Tables 2 and 4).

Although the IPCC method tends to produce higher mid-point estimates for total N_2O emissions, the ranges of IPCC and NEO emissions show overlap, and the IPCC range exceeds the NEO range (Fig. 3). For instance, the IPCC range for Dutch emissions amounts to 11–117 Gg N_2O-N y^{-1} (Table 2), while the NEO range is 13–70 Gg N_2O-N y^{-1} (Table 4). This is in line with the fact that the NEO method has been validated against Dutch research where possible, while the IPCC method is considered applicable to any country of the world and thus it is more uncertain. The relatively large ranges reflect the uncertainty in emission factors only.

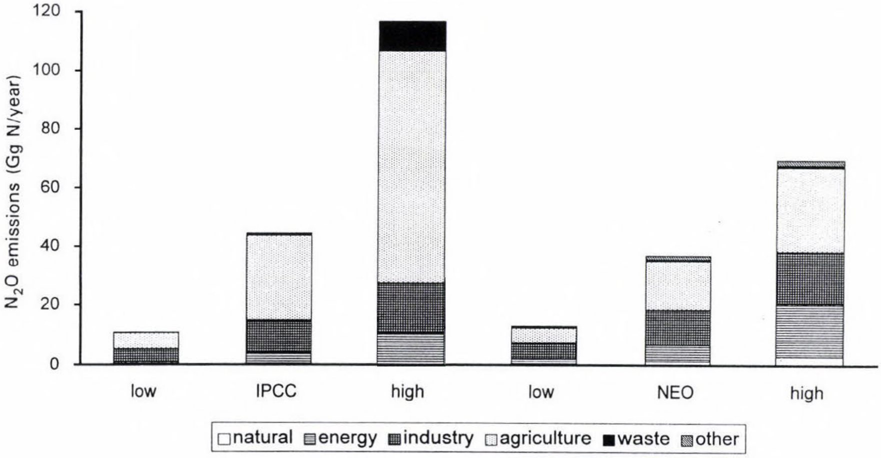

Fig. 2. Dutch 1990 emissions of N_2O estimated following the IPCC and NEO methods. Low and high estimates refer to ranges in emission factors (Tables 2 and 4).

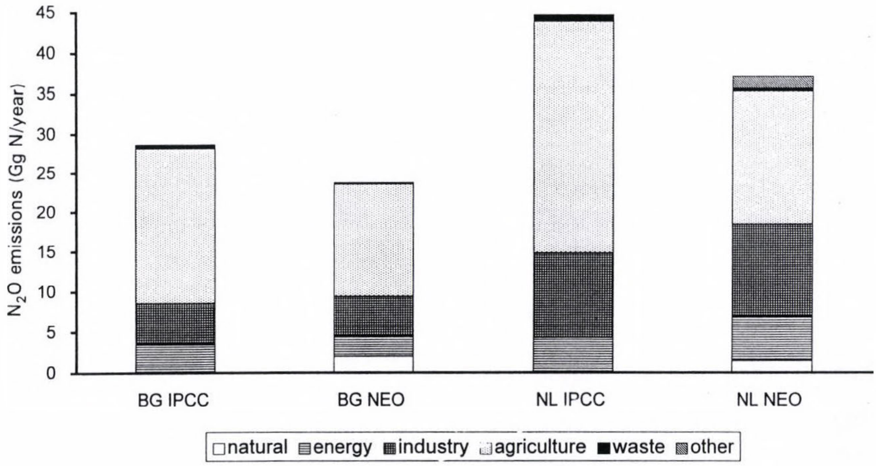

Fig. 3. Bulgarian 1988 and Dutch 1990 emissions of N_2O estimated following the IPCC and NEO methods.

The NEO method includes a number of sources that are not included in the IPCC method. These are natural emissions, enhanced background emissions from mineral soils, N_2O induced by NOx deposition, chemical industries other than nitric and adipic acid, atmospheric formation of N_2O, use in anaesthesia, enhanced emissions due to global warming and aquatic emissions due to non-agricultural N-inputs (see Fig. 3). On the other hand, the NEO method does not account for emissions resulting from crop residues.

Some sources are calculated in different ways in the two methods. For instance, N excretion by livestock in the Netherlands according to the IPCC method (780 Gg N) exceeds the NEO estimate (585 Gg N; *Van der Hoek*, 1994). As a result, there are differences between estimates for N_2O from manure in stables and manure applied as fertilizer. In addition, the enhanced background emissions are estimated differently, as well as emissions as a result of leaching. The net effect of this is that the IPCC estimate for agricultural emissions exceeds the NEO estimate by about 70% for the Netherlands and 40% for Bulgaria.

8. N_2O emissions: Bulgaria versus the Netherlands

Total N_2O emissions from Bulgaria are 29 (IPCC) and 24 (NEO) Gg N y^{-1} and from the Netherlands 45 (IPCC) and 37 (NEO) Gg N y^{-1}. Thus total anthropogenic emissions from the Netherlands are about 15 Gg N higher than those from Bulgaria (Figs. 1, 2 and 3). Dutch emissions exceed Bulgarian for the following sources: agriculture (3–9 Gg N), traffic (about 3 Gg N), nitric acid production (about 6 Gg N), and "other" emissions (about 2 Gg N). These differences mainly result from differences in human activities. For instance, nitric acid production in the Netherlands is about twice of that in Bulgaria. Traffic emissions in the Netherlands exceed those from Bulgaria not only because of a greater number of cars, but mainly because in the Netherlands 3-way catalysts tend to increase N_2O emissions to a larger extent than in Bulgaria.

Dutch agriculture gives rise to more N_2O production than the Bulgarian. This is partly a result of higher nitrogen input to soils in the Netherlands (922 Gg N y^{-1} according to the IPCC method) than in Bulgaria (624 Gg N y^{-1}) (Table 1). Similarly, the Dutch indirect agricultural N_2O emissions are about two times higher than those in Bulgaria. The agricultural N_2O in the Netherlands is largely related to manure produced by relatively large number of animals with relatively high per capita nitrogen excretion, and a relatively large fraction of manure produced in stables. Finally, there are no cultivated organic soils in Bulgaria, while in the Netherlands about 15% of the agricultural soils are classified organic. Organic soils tend to produce more N_2O than mineral.

The estimates for N_2O from stationary combustion vary considerably, mainly because for Bulgaria the IPCC and NEO methods differ (3.5 and 0.5 Gg N, respectively). This is a result of differences in the applied emission factors for coal combustion. In the NEO method 0.9 g N_2O-N GJ^{-1} is used, except for coal burning in boilers with fluidized bed combustors (FBC) when the emission factor is 26.7 g N_2O-N GJ^{-1}. This is a simplified interpretation of the IPCC Guidelines and partly based on Dutch research. In Bulgaria there is no FBC so that all NEO emissions from coal combustion are calculated using the low emission factor. The IPCC estimate for coal combustion in energy production was calculated using an emission factor of 0.5 g N_2O-N GJ^{-1}, and for combustion outside energy production 36.6 g N_2O-N GJ^{-1} (*Bogdanov*, 1995, 1996) was used. Clearly, validation of these emission factors is desirable.

The emissions of N_2O from mobile sources depend strongly on the presence of cars with 3-way catalyst control. In Bulgaria 3-way catalysts are not commonly applied, because of the absence of legislative regulations and the relatively old car fleet, with a considerable number of cars produced in former socialist countries. In the future, however, emissions from traffic in Bulgaria may increase when 3-way catalysts will be introduced.

9. Conclusions

The purpose of this study is:

(i) to apply both the IPCC and NEO methods to Bulgaria and the Netherlands,

(ii) to investigate differences between the NEO and IPCC methods and

(iii) to compare emissions from Bulgaria to emissions from the Netherlands.

This study shows that the NEO method can be applied to Bulgaria, although for some sources additional assumptions were necessary. These involve estimates for background emissions and emissions from waste water treatment. Further, data on N input to aquatic systems from industries were not available. Validation of the IPCC and NEO method for Bulgaria is difficult, because no experimental data on Bulgarian N_2O emissions exist. Nevertheless, it may be tentatively concluded that the NEO method is applicable to most regions of the world at Northern mid-latitudes, because the most important regional differences may be caused by climatic differences.

For both countries the IPCC method results in about 20% higher mid-point estimates for total emissions than the NEO estimates. The methods differ for several sources, but in particular for agriculture. The IPCC estimate exceeds the NEO estimate for both countries, despite the fact that the NEO method does not account for crop residues as source of nitrogen. The IPCC Guidelines used here (phase II Guidelines) result in higher agricultural emissions than the previous (phase I) IPCC Guidelines, in which agricultural emissions were estimated as a percentage of N input to soils only. For Bulgaria, for instance, the present estimates for agriculture (14 and 20 Gg N_2O-N y^{-1}) are 3–4 times higher than those based on the phase I IPCC Guidelines (*Bogdanov,* 1995, 1996). The Dutch estimates presented here (17 and 29 Gg N_2O-N y^{-1}) exceed the phase I estimate (2.4 Gg N) even by a factor of 7–10.

Annual emissions from the Netherlands exceed the Bulgarian emissions by about 15 Gg N y^{-1} (mid-point estimates). This is mainly a result of differences in human activities affecting emissions from agriculture, traffic and nitric oxide. A further comparison of emissions from Bulgarian to the Dutch situation reveals that:

(i) the emission factors used for estimating N_2O emissions from stationary combustion in Bulgaria need to be validated, because differences in emission factors used resulted in relatively large differences in estimated emissions from commercial boilers and fluidized bed combustion (FBCs),

(ii) emissions of N_2O from traffic are lower in Bulgaria than in the Netherlands, due to the low number of 3-way catalyst-equipped cars in Bulgaria,

(iii) indirect soil emissions of N_2O induced by atmospheric deposition of NO_x are relatively large in Bulgaria taking into account the total fuel consumption in both countries (further analysis of NO_x emissions would be necessary to validate these estimates),

(iv) enhanced background emission from soils are lower in Bulgaria than in the Netherlands, while the Bulgarian agricultural area exceeds the Dutch by more than a factor of two; this is a result of the absence of histosols in Bulgaria.

The uncertainties in the N_2O emission estimates are large compared to the differences between the mid-point values (Figs. 1, 2 and 3). These ranges only reflect the uncertainties in emission factors, not in activity data. The uncertainties could be reduced through experimental research. This holds for both countries, but for Bulgaria in particular, because there are no N_2O measurements available yet. In Bulgaria, measurements of N_2O emissions from agriculture would be particularly helpful. It is also recommended to establish specific Bulgarian values for annual nitrogen production by livestock, an in-country inventory of animal waste management systems, and a study on the fate of nitrogen in manure. In addition, a more precise estimate of N-flux in crop residues, especially through data for the residues removed from the fields and burned on site would be helpful, as well as an investigation of the practice in municipal, industrial and domestic waste water treatment, additional N-load to surface waters.

Acknowledgements—We would like to thank the International Agricultural Centre (Wageningen, the Netherlands) for financial support.

References

Baas, J., 1991: Literature review of nitrous oxide emissions from transport (in Dutch). *TNO-Rapport* R91/322. TNO Institute of Environmental Science. Delft, The Netherlands.

Baas, J., 1994: Nitrous oxide emissions from road transport in the Netherlands. *TNO-Report* R94/208. TNO Institute of Environmental Science. Delft, The Netherlands.

Bogdanov, S.B., 1995: GHG emissions in Bulgaria 1987-1993. *Report* for Bulgarian Case Study under US Country Studies Program, Sofia, Bulgaria.

Bogdanov, S.B., 1996: Inventory of GHG emissions in Bulgaria: 1987-1993. In *Greenhouse Gas Emissions Inventories (Interim Results from the U.S. Country Study Program)* (ed.: *B.V. Braatz*). Kluwer Academic Publishers, Dordrecht, The Netherlands, pp. 237-252.

Bouwman, A.F. and *Van der Hoek, K.W.*, 1991: Analysis of soil and water borne emissions of nitrous oxide and methane in the Netherlands. *RIVM Report,* No. 736301010. National Institute of Public Health and the Environment, Bilthoven, The Netherlands.

Bouwman, A.F., Van der Hoek, K.W. and *Olivier, J.G.J.*, 1995: Uncertainties in the global source distribution of nitrous oxide. *J. Geophys. Res. 100*, 2785-2800.

Bouwman, A.F., 1996: Direct emission of nitrous oxide from agricultural soils. *Nutrient Cycling in Agroecosystems 46*, 53-70.

Bowden, R.D., Melillo, J.M. and *Steudler, O.A.*, 1991: Effects of nitrogen additions on annual nitrous oxide fluxes from temperate forest soils in the northeastern United States. *J. Geophys. Res. 96,* 9321-9328.

Brumme, R. and *Beese, F.*, 1992: Effects of liming and nitrogen fertilization on emissions of CO_2 and N_2O from a temperate forest. *J. Geophys. Res. 97*, 12851-12858.

Ecetoc, 1994: Ammonia emissions to air in Western Europe. *Technical Report*, No. 26, Brussels.

FAO, 1990: *FAO Yearbook Production, Vol. 44.* FAO Statistic series 99. Rome, Italy.

Houghton, J.T., Meira Filho, L.G., Bruce, J., Hoesung Lee, Callander, B.A., Haites, E., Harris, N. and *Maskell, K.*, 1995: *Climate Change 1994. Radiative Forcing of Climate Change and an Evaluation of the IPCC IS92 Emission Scenarios*. Published for the Intergovernmental Panel on Climate Change, Cambridge University Press.

IPCC/OECD, 1995: *IPCC Guidelines for National Greenhouse Gas Inventories*. IPCC WGI Technical Support Unit, Bracknell, UK.

IPCC/OECD, 1997: *Revised 1996 IPCC Guidelines for National Greenhouse Gas Inventories (Phase II).* IPCC WG 1 Technical Support Unit, Bracknell, U.K. Nitrous oxide emissions from agriculture revised by *A. Mosier, C. Kroeze, C. Nevison, O. Oenema, S. Seitzinger, O. van Cleemput, L. Bakken, P. Bielek, S. Bogdanov, Y. Bonduki, A.F. Bouwman, R.A. Delmas, F.J. Dentener, R. Francisco, J. Freney, S. Frolking, P. Groffman, O. Heinemeyer, R. Karaban, L. Klemedtsson, P.A. Leffelaar, E. Lin, K. Minami, W.J. Parton, D.C. Parashar, R. Scholes, R. Sherlock, K. Smith, H.G. van Faassen, E. Veldkamp, G.L. Velthof* and *G.X. Xing*.

Kroeze, C., 1994: Nitrous oxide — emission inventory and options for control in the Netherlands. *RIVM Report* 773001004. National Institute for Public Health and the Environment, Bilthoven, The Netherlands.

Kroeze, C., 1995: Comparison of inventory methods for estimating national emissions of nitrous oxide (N_2O). *Időjárás 99*, 209-225.

Mosier, A.R., 1994: Nitrous oxide emissions from agricultural soils. *Fertilizer Research 37,* 191-200.

Mosier, A.R., Kroeze, C., Nevison, C. Oenema, O., Seitzinger, S. and *Van Cleemput, O.*,: Closing the global anthropogenic N_2O budget: nitrous oxide emissions through the agricultural nitrogen cycle. Accepted for publication in *Nutrient Cycling in Agroecosystems.*

Nevison, C.D., Esser, G. and *Holland, E.A.*, 1996: A global model of changing N_2O emissions from natural and perturbed soils. *Climatic Change 32*, 327-378.

Oenema, O., 1995: Direct nitrous oxide emissions in animal production: report of group II of the IPCC/OECD "N_2O Workgroup". Presented at the SENSE Symposium "Broeikaseffect en

Klimaatverandering: invloed van, en gevolgen voor landgebruik, ecosystemen en biodiversiteit". 17 November 1995. Wageningen, The Netherlands.

Prinn, R., Cunnold, D., Rasmussen, R., Simmonds, P., Alyea, D., Crawford, A., Fraser, P. and *Rosen, R.*, 1990: Atmospheric emissions and trends of nitrous oxide deduced from ten years of ALE-GAGE data. *J. Geophys. Res. 95,* 18369-18385.

RIVM, 1993: *National Environmental Outlook 3.* National Institute of Public Health and the Environment. Bilthoven, The Netherlands.

Safley, L.M., Casada, M.E., Woodbury, J.W. and *Roos, K.F.*, 1992: Global methane emissions from livestock and poultry manure. *US-EPA Report* No. 400/1-91/0458. Office of Air and Radiation, Washington D.C., USA.

Seitzinger, S.P., 1988: Denitrification in freshwater and coastal marine ecosystems: ecological and geochemical implications. *Limnol. Oceanogr. 33,* 702-724.

Seitzinger, S.P., 1990: Denitrification in aquatic sediments. In *Denitrification in Soil and Sediment* (eds.: *N.P. Revsbech* and *J. Sorensen*). Plenum Press, New York, pp. 301-312.

Spoelstra, H., 1993: N_2O emissions from combustion processes used in the generation of electricity. *Report* No. 10142-KES/MME 92-4029. KEMA Environmental Service, Arnhem, The Netherlands.

Steffens, G. and *Vetter, H.*, 1990: *Neue Faustzahlen über Nahrstoffgehalte und Nahrstoffanfall.* Landwirtsschaftsblatt Weser-Ems, 3.

Van Amstel, A.R., Albers, R.A.W., Kroeze, C., Matthijsen, A.C., Olivier, J.G.J. and *Spakman, J.*, 1994: Greenhouse gas emissions in the Netherlands 1990, 1991, 1992 and projections for 1990-2000. A background report for the National Communications of the Netherlands for the Climate Convention. *RIVM Report* No. 773001003. National Institute of Public Health and the Environment. Bilthoven, The Netherlands.

Van der Hoek, K.W., 1994: Methodology for calculating ammonia emissions in the Netherlands for the years 1990, 1991 and 1992 (in Dutch). *RIVM report* No. 773004003. National Institute for Public Health and the Environment. Bilthoven, The Netherlands.

Velthof, G.L. and *Oenema, O.*, 1994a: Effect of nitrogen fertilizer type and urine on nitrous oxide flux from grassland in early spring. In *Grassland and Society: Proceedings of the 15th General Meeting of the European Grassland Federation* (eds.: *L. 't Mannetje* and *J. Frame*). Wageningen, The Netherlands, pp. 458-462.

Velthof, G.L. and *Oenema, O.*, 1994b: Nitrous oxide emissions from grassland on sand, clay and peat soils in the Netherlands. In *Non-CO_2 Greenhouse Gases. Why and How to Control?* (eds.: *J. van Ham, L.J.H.M. Janssen* and *R.J. Swart*) Proc. of an International Symposium, 13-15 December 1993. Maastricht, The Netherlands. Kluwer Academic Publishers, London, pp. 439-444.

Vetter, H., Klasink, A. and *Steffens, G.*, 1989: Mist und Gülledüngung nach Mass. *VDLUFA-Schriftenreihe 19*, 41-66.

VROM, 1994: *Netherlands' National Communication on Climate Change Policies.* Prepared for the conference of parties under the Framework Convention on Climate Change. Ministry of Housing, Physical Planning and Environment. The Hague, The Netherlands.

IDŐJÁRÁS
Quarterly Journal of the Hungarian Meteorological Service
Vol. 101, No. 4, October-December 1997, pp. 261-273

Determination of precipitable water for a fixed site using *Global Positioning System* technique

Éva Borbás

Satellite Research Laboratory, Hungarian Meteorological Service,
P.O. Box 39, H-1675 Budapest, Hungary; E-mail: borbas@met.hu

(Manuscript received 1 July 1997; final form 19 August 1997)

Abstract—Water vapor plays an important role in atmospheric processes ranging from global climate change to micrometeorology, therefore its observation is essential for weather and climate research as well as operational weather forecasting. In addition the distribution of water vapor is highly variable in space and time and current numerical models require a better knowledge of this parameter. The resolution of conventional meteorological measurements (radiosonde, remote sensing observations) is limited both in time and space but new methods using data from the Global Positioning System (GPS) in meteorology could provide water vapor measurements as well as other atmospheric parameters such as temperature or pressure profiles with high spatial and temporal resolution. This paper reports about the application of GPS in meteorology and describes the methodology of deriving precipitable water vapor (PWV) from GPS processed data. Comparison with meteorological data (radiosonde, NOAA TOVS) and numerical weather prediction (NWP) model analyses are presented and it is shown that GPS method provides more accurate values of PWV than conventional measurements.

Key-words: ground-based GPS application, zenith tropospheric delay, zenith hydrostatic delay, zenith wet delay, precipitable water vapor.

1. Introduction

An important goal in weather prediction is to improve the accuracy of short-term cloud and precipitation forecast by creating a better initial state for the NWP model. One current limitation is the lack of precise information on the variability of the water vapor distribution both in time and space. *Kuo et al.* (1993) have shown that the assimilation of accurate and high resolution PWV data into a mesoscale model recovers the vertical structure of water vapor with much higher quality than that from statistical retrieval based on climatology and it has a positive impact on the short-range NWP.

A number of different methods have been developed to measure or to derive the vertical and horizontal distribution of water vapor. The radiosondes are in situ measurements providing good vertical resolution of humidity profiles (with accuracy of 3.5%) but because of their high costs, they are launched only twice a day at a limited number of stations. It is possible to estimate the integrated water vapor content (or precipitable water vapor) using a ground based upward looking water vapor radiometer (WVR). This instrument, which provides a good measurement accuracy, is used, in particular, by geophysicists to estimate the tropospheric effects on radio signals. The WVRs measure the background microwave radiation (actually the sky brightness temperature at two or more frequencies) produced by atmospheric water vapor and can estimate the integrated water vapor content along a given line of sight. The method, however, does not provide measurements under all weather conditions and the implementation of a fully meteorological operational system is not feasible. The space-based downward-looking radiometers providing a better spatial but poorer temporal coverage than the ground based instruments are better suited for meteorological application but do not satisfy the full requirement of current models. PWV can also be measured or derived remotely from both geostationary and polar orbiting satellites. Examples of such sounding instruments are the Visible-Infrared Spin Scan Radiometer (VISSR) Atmospheric Sounder (VAS) on NOAA GOES satellites (*Smith,* 1983) or the Tiros Operational Vertical Sounder (TOVS) on NOAA polar orbiting satellites. Their main common disadvantage is that derivation of PWV can be made accurately over cloud-free regions only. At the Satellite Research Laboratory of the Hungarian Meteorological Service humidity and temperature profiles are computed from TOVS data using an International TOVS Processing Package (ITPP) model (*Nieman and Achtor,* 1995) since 1992.

In addition to the above mentioned systems, there are also other space based (SSM/I, AMSU, etc.) and ground based (infrared and solar-optical radiometric technique) instruments used in the determination of PWV. This paper addresses a new and different promising method using the Global Positioning System (GPS).

In the 1970's the number of different navigation systems and associated costs have increased by a large amount. The US Department of Defense (DoD) has therefore decided to create a totally space based navigation system which was called Global Positioning System (*Hoffmann-Wellenhof et al.*, 1993). It was originally designed as a navigation and time transferring system but rapidly a number of other applications making use of the system emerged such as the meteorological one. The first GPS satellite (so-called PRN 4) was launched on 22 February 1978 (*Kleusberg et al.,* 1996). It was the first in a series of 11 so-called Block I satellites. Today satellite PRN 12 is the last of the Block I satellites still alive. The first satellite of the next generation (Block II) of the GPS satellites was launched in February 1989. Twenty-four Block II satellites are operational today. The GPS satellites which will replace the Block II's are the Block IIR's which have a design life of 10 years. The US GPS consists of 24 satellites orbiting the Earth at an altitude of 20200 km in 6 orbital planes (12 hour orbits), separated by about 60 degrees on the equator, and set with the inclination of about 55 degrees. Four to eight satellites (above 15° elevation) can be observed simultaneously from almost anywhere on the Earth at any time of the day.

There is also a Russian equivalent to GPS called Global Navigation Satellite System (GLONASS). The two systems are very similar, and it is possible to make use of both of them, resulting in a larger number of satellites and more options to chose the best positioning satellites to include in the derivation of the solutions. The combined system is called the Global Positioning and Global Navigation Satellite Systems (GNSS). The signals from the GLONASS satellites can be received since 1996 but the slight differences between the frequencies, altitudes etc. of satellites of the two systems result in the need for improvement in the receiving equipment (*Allan,* 1996). In this study only the data from the GPS (US) satellites were processed.

The GPS satellites transmit radio signals at 1.2 and 1.6 GHz through the Earth's atmosphere to the users equipped with GPS receivers. The ionosphere and the neutral atmosphere affect microwave transmission by slowing down the speed of the radio signals compared to that of the vacuum and curving the ray path. Both effects introduce propagation delays into the travel path length.

The ionospheric delay can be eliminated by using simultaneously two carrier frequencies because its refractivity depends on the frequency. However the neutral atmosphere is a non-dispersive medium for radio waves. The relative errors associated with the behavior of the neutral atmosphere have become more and more significant in the derivation of parameters as the space geodetic techniques were improved. To estimate and eliminate the delay caused by the troposphere especially by the highly variable water vapor above a GPS receiver, the geophysicists and geodesists have developed methods using a network of the ground-based GPS receivers. The delay caused by water vapor — called zenith wet delay (ZWD) — is nearly proportional to the amount of precipitable water vapor (PWV). A precise determination of ZWD and the knowledge of the functional relation between ZWD and PWV should allow the exploitation of a GPS network as a meteorological ground-based observation network for accurate, continuous determination of PWV fields. The application can be referred as "ground-based GPS meteorology" in opposition to "space-based GPS meteorology". In this paper after introducing and describing the techniques of both meteorological applications (Section 2), the evaluation of the ground-based GPS application and results of the test cases are presented and discussed for a fixed geographical site.

2. *GPS meteorology*

2.1 Space-based GPS meteorology

The branch of GPS meteorology using a GPS receiver spaced on board of a Low Earth Orbiting (LEO) satellite is referred as space-based GPS meteorology. The derivation method uses the radio occultation technique. The history of radio occultation technique started more than two decades ago and was used for studies of the atmospheres of other planets in our solar system. The related experiments have demonstrated the capability of the radio occultation technique to derive profiles of refractivity, neutral density, pressure and temperature for Venus (*Fjeldbo et al.* 1971), Mars (*Fjeldbo and Eshleman,* 1968), Jupiter (*Lindal et al.,* 1981) and some other planets as well as for the Earth.

The radio occultation technique for remote sensing of the neutral atmosphere uses the following approach: the radio signal propagates from the GPS transmitter to the LEO receiver while it traverses the atmosphere from the ionosphere to the limb of the Earth as the satellite moves in its orbits (*Fig. 1*). The propagation path of the electromagnetic wave will be curved and slowed down, as it was mentioned in the previous section. As there is a unique relationship between the total refractive bending angle (α) and the atmospheric refractive index (or refractivity) (*Melbourne et al.,* 1994), the refractivity for each layer can be determined from the measured angle. But the atmospheric refractivity (N) can be approximated (*Smith* and *Weintraub*, 1953; *Thayer,* 1974) by

$$N = 77.6 \frac{P_d}{T} + 3.73 * 10^5 \frac{P_w}{T^2}, \tag{1}$$

where P_d is the partial pressure of the dry air (in hPa), T is the temperature of the atmosphere (in K) and P_w is the partial pressure of the water vapor (in hPa) in a layer. The effect of humidity and temperature are not separable. The humidity can be retrieved only if the temperature is known and alternatively the temperature can be accurately (better than one degree Kelvin) determined only if the humidity is known, or using the equation of the states for arid region of the neutral atmosphere: stratospheric temperatures globally and upper tropospheric temperatures at middle and high latitudes (*Gorbunov* and *Sokolovskiy*, 1993).

The first LEO satellite with a small radio receiver was launched on 3 April, 1995. More information about this and the space-based GPS application can be read in the report of the GPS/MET team of NCAR (*Ware et al.*, 1994) or in an ESA contract report (*Høeg et al.,* 1996).

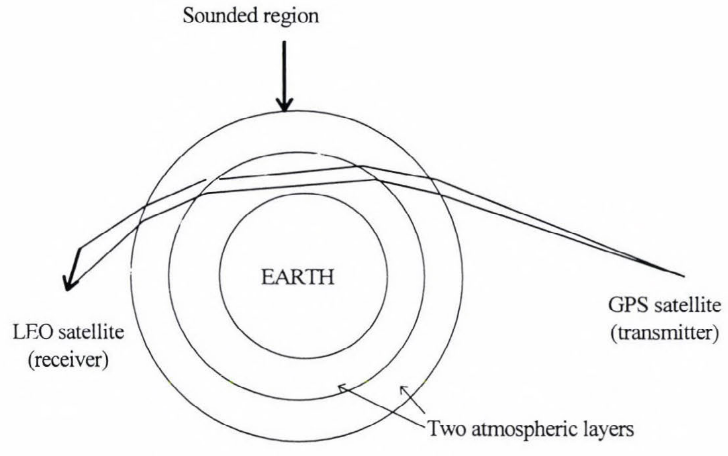

Fig. 1. The radio occultation technique.

2.2 Ground-based GPS meteorology

The radio signals, received by a ground-based GPS receiver, are delayed by water vapor and dry gases of the neutral atmosphere. For this reason the total tropospheric delay (TD) can be partitioned into the wet delay (WD), which is a function of the water vapor distribution and the hydrostatic delay (HD):

$$TD = HD + WD. \tag{2}$$

HD is not considered as dry delay because, unlike dry gases, it includes the nondipole components of the refractivity values of the water vapor. Both delays are the smallest for paths from the zenith direction and increase approximately inversely with the sine of the elevation angle. The mapping function describes the dependence on elevation angle (*Davis et al.*, 1985). The typical value of the HD is 2.3 m at the sea level in the zenith direction and it is about 90 percent of the total tropospheric delay (TD). The value of the zenith wet delay (ZWD) can be less than 1.0 cm in arid regions and its maximum can reach about 40.0 cm in humid areas.

Elgered et al. (1991) used the following equation in an adopted model for the determination of zenith hydrostatic delay (ZHD):

$$ZHD = \frac{(2.2779 \pm 0.0024)\,P_s}{1 - 0.00266\cos 2\lambda - 0.00028\,H}, \tag{3}$$

where P_s is the total pressure (in hPa) at the Earth's surface, the denominator is the variation of the gravitation acceleration with the latitude (λ) of the station and the height (H) above the ellipsoid. Finally, the precipitable water vapor can be computed by the equation

$$PWV = k\,ZWD,$$

with

$$k = \frac{10^6}{(\rho_w R_v (k_3/T_m + k_2^{/}))},$$

where ρ_w is the density of water, R_v is the specific gas constant for water vapor, $k_2^{/} = 22.1 \pm 2.2$ (K/hPa) and $k_3 = (3.739 \pm 0.0012)\ 10^5$ (K^2/hPa) (*Bevis et al.*, 1994). The weighted mean temperature of the atmosphere (T_m) is defined (*Davis et al.,* 1985) as

$$T_m = \frac{\int (P_v/T)dz}{\int (P_v/T^2)dz}, \tag{4}$$

where P_v is the partial pressure of dry air and T is the absolute temperature. T_m can be estimated by $T_m = 70.2 + 0.72\ T_s$ (K) (*Bevis et al.*, 1992), where T_s is the surface temperature, or computed from a numerical weather prediction model which predicts the three dimensional distribution of temperature.

The zenith tropospheric delay has to be determined or estimated and very accurate meteorological measurements are necessary on site to derive the PWV at the GPS site using the above described GPS technique.

Originally a number of methods were developed to estimate and to eliminate the effects of tropospheric delay on GPS signals. The first and simplest method computes the wet (WD) and hydrostatic delay (HD) from surface pressure (Eq. (3)), temperature and humidity measurements using an atmospheric mapping function (*Saastamoinen*, 1972). This method is very good for the estimation of the ZHD but as ZWD is weakly related to the meteorological surface conditions, it results in bad estimation for our purpose. To avoid the extreme meteorological conditions (inversion, convection), meteorological data of a standard atmosphere are usually used in this method. An alternative method provides the wet delay using Water Vapor Radiometers or radiosondes to measure and determine the precipitable water. The routine operation of these instruments is expensive and WVR is not an "all-weather" instrument. A third method *estimates* the wet delay (or the residual zenith delay = actual ZD - calculated ZD) directly from the GPS data themselves of a network as a part of the overall least squares inversion for the coordinates of the GPS receivers, the orbital parameters of the GPS satellites, and other geodetic parameters of interest ("deterministic" approach). This method assumes that the ZWD is constant for an interval and hence it causes some constraints on ZWD values, and keeps them within reasonable bounds. Finally, the residual ZD can be estimated by a stochastic model using the Kalman filtering technique where the predicted value will be a time-dependent parameter. The stochastic filtering of the tropospheric delay showed very good results compared to the direct WVR measurements (*Bevis et al.*, 1992). The research group at Jet Propulsion Laboratory was the first to adopt a stochastic estimation method for atmospheric modeling within their GIPSY/OASIS GPS processing package (*Webb* and *Zumberge,* 1993). But a number of GPS processing packages still include the deterministic (Bernese, GAMIT, etc.) rather than the stochastic approach like in the models GIPSY and GAS (*Stewart et al.*, 1995).

2.2.1. Sources of errors

Bevis et al. (1994) showed that the relative error in k depends on the relative error in T_m which can be predicted from only the surface temperature (see the equation above) with a relative rms error of about 2% and from the NWP model with a relative rms error of 1%. Thus the estimation of PWV from ZWD causes a very little error in this process, it introduces errors of less than 5%. The hydrostatic delay can be determined better than 1 mm if the barometer is well calibrated (<0.3 hPa). The hydrostatic delay, however, can be affected by atmospheric dynamics which causes errors of less than 1% (23 mm). Additional errors can be caused by many other conditions as the effects of multipath signals, the effects of incorrect modeling of the elevation angle, the effects of the assumption of the azimuthal symmetry, clock errors etc., but these errors are not significant. *Gutman et al.* (1995) showed that the differences between PWV calculated by using precise orbits and rapid orbits are negligible furthermore there are not significant differences between the results obtained by different GPS processing packages. Thus the major source of the errors in the determination of PWV results from errors of geodetic processing of the GPS data.

3. Determination of PWV values from various measurements for comparison

The aim of the study is to investigate the quality of GPS-derived PWV data for the only Hungarian permanent GPS station, located at Penc (47.789°E; 19.281°N; 247 meters). The data from which PWV amounts can be computed and are available at the Hungarian Meteorological Service are the measurements of the European radiosonde stations twice a day, NOAA TOVS radiances four times a day and forecasts and analyses of a Numerical Weather Prediction model every three hours. The GPS derived, two hourly zenith tropospheric delays were provided by the Central European Regional Geodynamic Project (CERGOP) Data Center at the Institute of Space Research, Department of Satellite Geodesy in Graz (*Pesec* and *Stangl*, 1995). The comparisons of various derived PWV were made above the GPS station Penc during the period April-May 1996.

The CERGOP Data Center computes zenith tropospehric delay (ZTD) estimates every two hours as a part of the least squares adjustment of a Central European GPS network by using the Bernese software (*Rothacher et al.*, 1990). The network contains 15 Central European GPS sites and the orbits are rapid orbits obtained from the CODE (Center for Orbit Determination in Europe) Center of the International GPS Services for Geodynamics (IGS) in Bern with a three or four day time gap. Because of the "deterministic" approach, the zenith delays are constant during the estimation interval. The baselines between the stations of the network are not too long (less than 500 km), so the receivers view the same satellite at almost the same elevation angles, causing the ZTD estimates to be highly correlated. Therefore the PWV amounts computed from the Central European Network can be considered as relative values. Some techniques are developed to obtain absolute ZTD or PWV amounts. A few other GPS stations need to be added to the network to introduce baselines to be more than 500 km (absolute technique) (*Duan et al.*, 1996) or a Water Vapor Radiometer should be set at the reference station to determine the unknown bias to be applied to the whole network (the bias does not vary in space). The latter method is called WVR levering (*Businger et al.*, 1996).

PWV values were computed and interpolated from the radiosonde data of the European region using linear interpolation with distance-dependent weights. The data of a radiosonde station were considered only if the distance between the GPS site and the radiosonde station was less than 1000 km.

Precipitable Water amounts from NOAA/TOVS data were derived by using the International TOVS Processing Package (ITPP) 5.0 developed at the Cooperative Institute for Meteorological Satellite Studies (CIMSS). The PWV data were interpolated from the values of the nearest clear sky pixels.

The numerical weather prediction (NWP) model which was used in this study is a 12 σ level, primitive equation, limited area model (56×48 grid points, $d \sim 90$ km) developed at the Swedish Meteorological and Hydrological Institute (*Undén*, 1982). The PWV data were interpolated from the four nearest grid points. The model provides 36-hour predictions with three hour analyses.

4. Results

The bias, standard deviation, and rms deviation of the differences between the various PWV products derived from the different measurements and NWP analyses are summarized in *Table 1*. During the study we assumed that the radiosonde-derived PWV values provided the best data sets. However it should be noted that these values could have been improved using the surface meteorological data in the computation scheme. Referring to the comparisons with radiosondes, the GPS-derived PWV data were better than the TOVS-derived and the NWP PWV amounts. It can also be seen that in the future, further investigations are necessary to figure out the reason of the very high NWP PWV values. The first cell of the table shows that the GPS derived values underestimate the radiosonde PWV amounts (bias is –0.6 mm), which can prove that GPS PWV data are relative values correctable by using the absolute technique or WVR levering technique (see in Section 3).

Table 1. Bias, standard deviation and rms deviation of differences between TOVS-, GPS- and radiosonde-derived precipitable water amounts for April–May 1996

mm		RAOBS	NWP	NOAA-TOVS
GPS	bias	-0.664	-3.140	-1.468
	stdev	1.465	4.243	3.049
	rms	1.610	5.285	3.388
No. of cases		**83**	**153**	**81**
RAOBS	bias		-3.117	-1.422
	stdev		4.173	4.700
	rms		5.217	4.916
No. of cases			**116**	**38**
NWP	bias			2.297
	stdev			4.794
	rms			5.323
No. of cases				**72**

Comparisons of GPS-derived PWV values to radiosonde derived ones at the Penc site for Spring 1996 are shown in *Fig. 2*. The three plots indicate that the GPS derived PWVs follow the trend shown by radiosonde values very well. The reason for the lack of GPS PWV values on the plots is the lack of on-site meteorological observations at the GPS station. The on-site meteorological measurements at permanent stations are not too wide-spread yet or the collection of these types of data is not performed for the moment (but it is currently increasing). This is the reason why it was interesting to examine the effect of using the interpolated surface data from a meteorological observation network instead of using measured values in the PWV derivations (*Table 2*). The use of interpolated meteorological data would introduce an rms error not higher than 0.5 mm in the case of the Penc site. This error depends on the level of the accuracy of the meteorological data, the not well calibrated barometers, and also the high difference between the altitudes of the GPS antenna and the barometer. The bias (–0.4 mm) shows that interpolation underestimates the observation.

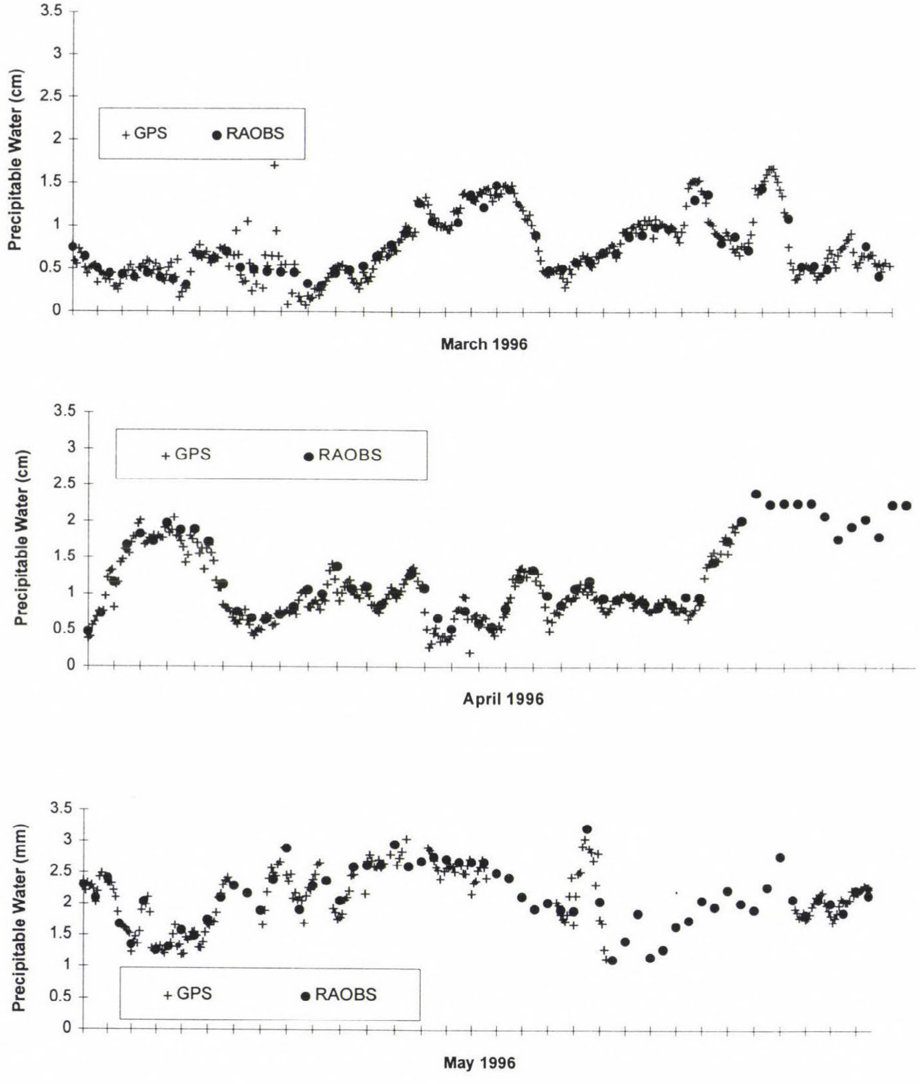

Fig. 2. Comparison of GPS-derived precipitable water amounts to radiosonde-derived values for Spring 1996 at Penc GPS station.

Table 2. Comparison statistics between the GPS-derived PWV values (mm) computed with observed meteorological data and with interpolated ones from the European meteorological observation network

Number of cases	bias	stdev	rms
491	-0.423	0.233	0.483

Our aim was also to examine the variability of the PWV data using a shorter estimation interval in the processing. The scientists of the Satellite Geophysical Observatory at Penc performed 30 minute ZTD estimations during the time period 15 to 18 March 1996. In the computation they used measurements taken at two GPS sites (Penc, Graz (Austria), baseline about 240 km), precise CODE orbits and the Bernese software. Because of the deterministic approach, the PWV values are constants in the intervals. The comparison of the 30 minute PWV amounts with the two-hourly one, using the estimates provided by the Graz center, is presented on *Fig. 3*. It can be observed that the distribution of water vapor is highly variable in time and choosing a 30 minute time interval (or less than 30 minutes) would provide more and useful information about the water vapor amount.

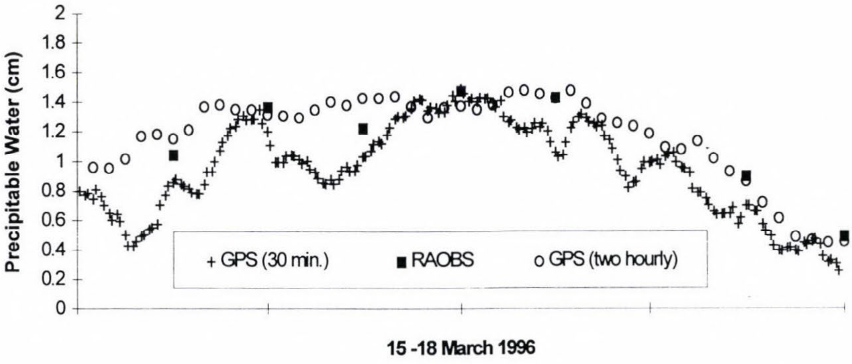

Fig. 3. The use of different time intervals (30 minutes and two hours) in the GPS processing to obtain precipitable water amounts. Comparison to each other and to the radiosonde-derived PWV values during the time period between 15 to 18 March 1996 at Penc site.

5. Conclusions and future plans

In this study we examined the quality of GPS-derived precipitable water amounts. For this reason, we compared them to values derived from other meteorological measurements and NWP analyses or forecasts for April and May 1996. It is shown that the GPS method provides more accurate values of precipitable water amounts than the NOAA TOVS radiances or NWP analyses and forecasts and the method has a much better temporal resolution. The use of interpolated meteorological data instead of on-site measurements in the computation of GPS PWV values was also examined. It introduced an 0.5 mm rms error in case of Penc site.

The results showed that GPS technique can provide accurate estimates of PWV with sub-hourly temporal resolution but the current problem is that results are not available in real time. The main problem of getting near real time PWV estimates is the acquisition of the real time precise orbit data. The real time precise orbit processing is currently under development.

In the future we are planning to improve the accuracy of the GPS derived PWV data by computing the T_m mean temperature from the NWP analyses. Our main purpose is to examine the impact of the GPS-derived PWV data on the NWP analyses and on the forecast, hence we intend to assimilate accurate GPS-derived PWV values of an European GPS network into the LAM NWP model which was adapted from the Swedish Meteorological and Hydrological Institute. For this purpose, we will have to apply the method which was described in this paper for a more extended European GPS network.

Acknowledgements—I would like to acknowledge the role of, and thank the scientists at the Satellite Geodesy Observatory in Penc and the Department of Satellite Geodesy at the Institute for Space Research in Graz for providing the processed GPS data. This study was partially supported by State Scientific Research Fund (OTKA F 015963) and by the National Committee for Technological Development (OMFB TP 063).

References

Allan, D.W., 1996: Harmonizing GPS and GLONASS. *GPS World 7*, No. 5, 51-53.

Bevis, M., Businger, S., Herring, T.A., Rocken, C., Anthes, R.A. and *Ware, R.H.*, 1992: GPS meteorology: Remote sensing of atmospheric water vapour using the global positioning system. *J. Geophys. Res. 97*, 15787-15801.

Bevis, M., Businger, S., Herring, T.A., Anthes, R.A., Rocken, C., Ware, R.H. and *Chiswell, S.R.*, 1994: GPS meteorology: Mapping zenith wet delay onto precipitable water. *J. Appl. Meteor. 33*, 379-386.

Businger, S., Chiswell, S., Bevis, M., Duan, J., Anthes, R.A., Rocken, C., Ware, R.H., Exner, M., Hoven T., and *Solheim, F.S.*, 1996: The promise of GPS in atmospheric monitoring. *Bull. Amer. Meteorol. Soc. 77*, 5-18.

Davis, J.L., Herring, T.A., Shapiro, I.I., Rogers, A.E. and *Elgered, G.*, 1985: Geodesy by radio interferometry: Effects of atmospheric modelling errors on estimates of baseline length. *Radio Sci. 20*, 1593-1607.

Duan, J., Bevis, M., Fang, P., Bock, Y., Chiswell, S., Businger, S., Rocken, C., Solheim, F., VanHove, T., Ware, H.R., McClusky, S., Herring, T.A. and *King, R.W.*, 1996: GPS meteorology: Direct estimation of the absolute value of the precipitable water. *J. Appl. Meteor. 35*, 830-838.

Elgered, G., Davis, J.L., Herring, T.A. and *Shapiro, I.I.*, 1991: Geodesy by radio interferometry: Water vapor radiometry for estimation of the wet delay. *J. Geophys. Res. 96*, 6541-6555.

Fjeldbo, G. and *Eshleman, V.R.*, 1968: The atmosphere of Mars analyzed by integral inversion of the Marine IV occultation data. *Planet. Space Sci. 16*, 1035-1059.

Fjeldbo, G., Kliore, A.J. and *Eshleman, V.R.*, 1971: The neutral atmosphere of Venus as studied with the Marine V radio occultation experiments. *Astnonom. J. 76*, 123-140.

Gorbunov, M. E. and *Sokolovskiy, S.V.*, 1993: Remote sensing of refractivity from space for global observations of atmospheric parameters. *Report*, No. 119. Max-Planck-Institute for Meteorology, Hamburg, Germany.

Gutman, S.I., Wolfe, D.E. and *Simon, A.*, 1995: Development of an operational water vapor remote sensing system using GPS: a progress report. *FSL Forum*, December 1995, 21-32.

Hoffmann-Wellenhof, B., Lichtenegger, H. and *Collins, J.*, 1993: *GPS-theory and Practice* (second edition). Springer-Verlag, Wien, New York.

Høeg, P., Hauchecorne, A., Kirchengast, G., Syndergaard, S., Balloul, B., Leitinger, R. and *Rothleitner, W.*, 1996: Derivation of atmospheric properties using radio occultation technique. *DMI Scientific Report*, 95-4. Danish Meteorological Institute, Copenhagen, Denmark.

Kleusberg, A. and *Teunissen, P.J.G.*, 1996: *GPS for Geodesy*. Lecture Notes in Earth Sciences 60. Springer-Verlag, Berlin, Heidelberg.

Kuo, Y.-H, Guo, Y.-R. and *Westwater, E.R.*, 1993: Assimilation of precipitable water measurements into a mesoscale numerical model. *Mon. Wea. Rev. 121*, 1215-1238.

Lindal, G.F., Wood, G.E., Levy, G.S., Anderson, J.D., Sweetnam, D.N., Hotz, H.B., Buckles, B.J., Holmes, D.P., Doms, P.E., Eshleman, V.R., Typer, G.L. and *Croft, T.A.*, 1981: The atmosphere of Jupiter: An analysis of the Voyager radio occultation measurements. *J. Geophys. Res. 86*, 8721-8727.

Melburne, W.G., Davis, E.S., Duncan, C.B., Hajj, G.A., Hardy, K.R., Kursinski, E.R., Meehan, T.K., Young, L.E. and *Yunck, T.P.*, 1994: The application of spaceborn GPS to atmospheric limb sounding and global change monitoring. *JPL Publication*, 94-18, Pasadena, CA, USA.

Nieman S. and *Achtor, T.*, 1995: *ITPP-5.0 User Guide*. Cooperative Institute for Meteorological Satellite Studies, University of Wisconsin-Madison. ftp://winds.ssec.edu/www/tovs/userman.-html.

Pesec, P. and *Stangl, G.*, 1995: Current status of the CERGOP Processing Center Graz. *Proc. of the 3rd CERGOP working conference, Sződliget, Hungary, 8 May 1995 and 3rd International Seminar on "GPS in Central Europe", Penc, Hungary, 9-11 May, 1995,* 101 p.

Rothacher, M., Beutler, G., Gurtner, W., Schildknecht, T. and *Wild, U.*, 1990: *Documentation for Bernese GPS Software Version 3.2.* CODE Analysis Center of IGS, Univ. of Bern, Switzerland.

Saastamoinen, J., 1972: Atmospheric correction for the troposphere and stratosphere in radio ranging of satellites. In *The Use of Artificial Satellites for Geodesy. Geophys. Monogr.* Ser. 15. American Geophys. Union, Washington D.C., 247-251.

Smith, E.K. and *Weintraub, S.*, 1953: The constants in the equation of atmospheric refractive index at radio frequencies. *Proc. of the Institute of Radio Engineers 41,* No. 8, 1035-1037.

Smith, W.L., 1983: The retrieval of atmospheric profiles from VAS geostationary radiance observations. *J. Atmos. Sci. 40,* 2025-2035.

Stewart, M.P., Foulkes, G.H., Ochieng, W.Y. and *Shardlow, P.J.*, 1995: GAS: GPS Analysis Software, Version 2.32. *User Manual, Publication IESSG.* The University of Nottingham, United Kingdom.

Thayer, D., 1974: An improved equation for the radio refractive index in air. *Radio Sci. 6,* 803-807.

Undén, P., 1982: The Swedish limited area model. *SMHI Report,* RMK 35. Swedish Meteorological and Hydrological Institute, Stockholm.

Ware, R.H., Exner, M., Herman, B.M., Kuo, Y.-H., Meehan, T.K. and *Rocken, C.*, 1994: *Summary: GPS/MET Program, Phase I: Proof of Concept.* GPS/MET Workshop, NOAA, Boulder, USA, September 1994.

Webb, F.H. and *Zumberge, J.F.*, 1993: An introduction to the GIPSY/OASIS-II. *JPL Publ. D-11088,* Jet Propulsion Laboratory, Pasadena, California.

IDŐJÁRÁS
Quarterly Journal of the Hungarian Meteorological Service
Vol. 101, No. 4, October–December 1997, pp. 275–288

Measurement of mean stomatal resistance in maize

A. Anda, J. Páll and **Zs. Lőke**

Pannon University of Agricultural Sciences, Georgikon Faculty of Agronomy, P.O. Box 71, H-8361 Keszthely, Hungary; E-mail: and5536@ella.hu

(Manuscript received 26 May 1997; final form 15 September 1997)

Abstract—Field trial on maize stomatal resistance behavior was carried out at the research area of the Pannon Agricultural University of Keszthely, Hungary in the growing seasons of 1992–1996. The measurements had two purposes: first the investigation of the divergence in stomatal resistance of two epidermises in opened maize stand (May and June) and the second goal was to map the distribution of stomatal resistance inside a leaf and, later on, within a well developed maize plant. To verify mean stomatal resistance assumption a modified model of *Goudriaan* (1977) was used. Agreement between the simulated and measured resistances of two different water supply levels was quite good (8–12%), but only on completely clear days. At disturbed radiation conditions the differences between measured and simulated values sometimes exceeded 30%. To improve results more investigation is needed on maize stomatal resistance, mainly under variable radiation conditions.

Key-words: stomatal resistance distribution, resistance simulation, maize, modeling.

1. Introduction

The climate change in the past decades in the Carpathian basin resulted in about 10% decrease in yearly rainfall sum drawing the attention of researchers and farmers to the importance of water in the soil-plant-atmosphere continuum. There are several methods to investigate water supply state of crops; measuring precipitation amounts or available soil moisture from the most simple gravimetrical way to the application of more or less sophisticated instruments (for example neutron probe) etc. As the purpose of the study is tending towards plant-water relations, those measurements aimed directly at plant behavior must take priority. One of the plant features being in direct connection with plant water supply is the stomatal resistance. According to the importance of diffusive resistances in plant water balance, huge amount of papers dealt with its application together with the arising problems when it is used in field trials. Our goal was to complete earlier information about maize stomatal resistance behavior in field conditions. Parallel with resistance measurements we tried to interpret resistance results as well.

2. *Theoretical consideration*

The transpiration rate (E) in the simplest form expressed by Fick's law of diffusion is the ratio of the rate of gradient of water vapor from the intercellular spaces inside the leaf to the atmosphere (ΔW) to the sum of resistances on the way of water from the soil to the open air (Σr):

$$E = \frac{\Delta W}{\Sigma r}. \tag{1}$$

Since the air in intercellular spaces is assumed to be saturated, the transpiration driving force (ΔW) is equal to the difference between saturation vapor pressure at given leaf temperature (w_2) and actual vapor pressure of the ambient air (w_1):

$$\Delta W = (w_2 - w_1). \tag{2}$$

Because of the complexity of diffusive resistances occurring on water pathway from the soil to the air, the approach of calculating the denominator of fraction (Eq. (1)) is not as simple as calculation of ΔW. Soil moisture content determines hydraulic conductivity of the soil, whose inverse is the soil resistance (r_{soil}). In moist soils the r_{soil} is considered to be very small. Plant water uptake depends on the extent of root system (r_{root}) and sap movement of the xylem's vascular system (r_{xylem}). Roots are supposed to offer the largest resistance of the whole soil-plant-atmosphere system. The stem together with leaves nearly matches the resistance of roots. In leaves the water vapor diffuses from wet mesophyll cell walls surrounding the intercellular air spaces to the stomata, to "intercellular windows" allocated between two specialized guard-cells. Resistances of cuticle (r_{cu}) are in a parallel circuit with stomatal resistance (r_s) at the whole leaf resistance (r_{leaf}) calculation:

$$\frac{1}{r_{leaf}} = \frac{1}{r_{cu}} + \frac{1}{r_s}. \tag{3}$$

When stomas are open, r_{cu} is much higher than r_s, for this reason its value used to be ignored. Practically at amphistomatous plants the determination of true cuticular resistance is very complicated (almost impossible).

Stomatal resistance consists of individual but hardly approachable parts connected in series:

$$r_s = r_m + r_i, \tag{4}$$

where r_m is the resistance of mesophyll cell walls, and r_i is the resistance of intercellular spaces.

Using a theoretical consideration resistance of intercellular spaces is very small. The neglect of this component involves an error of 2–5% in the total r_s (*Kozlowsky,* 1976). Determination of r_m is difficult and a considerable uncertainty is still exist. Under normal outdoor conditions "general" resistance of mesophyll cell walls was assumed to be about 0.2 sec/cm (neglecting this means a 5% error at stomatal resistance estimation). As nowadays there is no way to measure r_s components distinctly, when porometer is applied the measured resistance is assumed to be equal to stomatal resistance. On the pathway of water vapor after leaving leaf surface 2 other resistances have left; resistance of boundary layer (r_b) and of turbulent air (r_a). These latter two are calculated from measuring plant (leaf) dimensions and wind characteristics.

Amphistomatous plants have two evaporating surfaces with more or less different resistances on abaxial (r_{su}) and adaxial (r_{sl}) leaf-sides being connected in parallel:

$$\overline{r_s} = \frac{r_{su} r_{sl}}{r_{su} + r_{sl}}. \tag{5}$$

In case of maize Eq. (5) must be applied during May and June. Later on measurement at one side is enough to characterize mean stomatal (leaf) resistance as the number of stomata is almost the same at both leaf surfaces.

Hence the key resistance to plant water loss is stomatal resistance — except when canopy is wet, — *Monteith* (1965) suggested to initiate the concept of canopy or surface resistance (r_c) characterizing water loss of the whole plant stand:

$$r_c = W_0/E \cong \overline{r_s}/LAI \quad \text{or} \quad r_c = \overline{r_s}/2\,LAI, \tag{6}$$

where W_0 is the vapor density deficit for given canopy surface temperature, $\overline{r_s}$ is the mean stomatal resistance for the whole plant, *LAI* is the leaf area index.

Choice depends on leaf stomatal distribution; at amphistomatous plants the second version is appropriate. One of our aims connected to Eq. (6), were to find the probable place of "mean stomatal resistance" inside a leaf and a fully developed maize plant.

3. Instrumentation to measure stomatal resistance and test model description

There are three different types of diffusion porometer (*Table 1*) to measure stomatal resistances (*Pearcy et al.,* 1991):

(1) The earliest porometers are the transient type ones, the closed chambers attached to the leaf. They measure "response" time required to increase humidity between two selected categories.

(2) Null-balance porometers keep the chamber humidity constant by introducing a varied flow of dry air into the chamber to balance the water vapor being lost by transpiration.

(3) Constant flow porometers measure a steady-state increase in humidity at constant air mass introduction after closing the leaf into the chamber.

Table 1. Comparison of different porometer types

Porometer type	Advantages	Disadvantages
Transient	Relatively simple to use Cheap Very good for "higher" resistances	Leaf size and shape limitations High temperature response Laborious calibration necessity Errors due to water sorption
Null-balance	Minimum water sorption Easier calibration Wide variety of leaf shape and size Best for "lower" resistances Complexity	Expensive
Constant flow	Both CO_2/H_2O exchange results in the same time	Error at high difference in ambient humidity (water absorption or desorption) Price increase (extra IR gas analyzer!) Less portable

In our experiments we applied an improved version of transient porometers manufactured by Delta T Devices in Great Britain (version AP 4). The AP 4 porometer has got a capacitance type humidity sensor, that makes possible more precise transit time determinations. The manufacturer applied new materials (polypropylene etc.) to minimize vapor sorption in sensor head. There is an extra (built up) microprocessor connected to the instrument that helps to achieve easy repeatable and considerably quick calibration results increasing the reliability of the improved porometer version.

The calibration of porometers has of primary importance because its accuracy determines the validity of all the resistance measurements. In most cases (in case of AP4 type porometer also) the following equation is adopted to construct a known resistance value:

$$r_s \text{ (sec/cm)} = \frac{L}{\alpha} 4A\left(Lo + \frac{\pi d}{8}\right) / \alpha n \pi d^2, \tag{7}$$

where L effective diffusion pathlength,
α diffusivity of water vapor at given temperature,
Lo actual length of each hole (on calibration plate),
A aperture area of the vapor cup,
n number of holes,
d diameter of the holes.

To test our field stomatal resistance observations a modified version of the Crop Simulation Model of *Goudriaan* (1977) was used. Modification was made by *Chen* (1984). Basis of assumption of stomatal resistance simulation is that mass transport processes — both water vapor and CO_2 — occur via stomata, so that the ratio between their resistances is equal to the ratio between their diffusivities. In case of maize plant a linear relationship exists between net CO_2 assimilation and inverse leaf resistance at constant CO_2 concentration of substomatal cavity. This connection served to simulate the leaf resistance, since net CO_2 assimilation can be deducted precisely from the absorbed short wave radiation *(Goudriaan,* 1977). Exceeding the saturation point of CO_2 assimilation (200 J m^{-2} s^{-1} for sunny maize leaves) the leaf resistance approaches its minimum value *(Stiger et al.,* 1977). Rate of net CO_2 assimilation was considered empirically by *Van Laar et al.* (1977) as follows:

$$F = (F_m - F_d)\,[1/\exp(R_v \varepsilon / F_m)] + F_d, \tag{8}$$

where F_m maximum rate of net assimilation,
F_d dark respiration,
R_v absorbed short wave radiation (per LAI),
ε slope of the curve of F–R_v at low light intensities, *or* efficiency (17.2×10^{-9} kg/J light in maize).

At calculation of F_m the influence of leaf age and ambient CO_2 concentration were simplified and their average values were applied. Dependence of leaf temperature was considered as a dependence on ambient air temperature. Dark respiration was at about –0.1 of F_m (*Goudriaan*, 1977). To calculate maize leaf (stomatal) resistance Eq. (8) can be written as:

$$F = \frac{1.83 \times 10^{-6} (C_e - C_r)}{1,66 r_{leaf} + 1.32 r_{b,h}} \quad \Rightarrow \quad r_{leaf} = \frac{1.83 \times 10^{-6} (C_e - C_r)}{1.66\, F} - 0.795, \qquad (9)$$

where $r_{b,h}$ boundary layer resistance for heat,
1.66 is the ratio between diffusivities (for CO_2 and H_2O),
1.83×10^{-6} converts CO_2 concentration into kg CO_2/m^2 at 20°C,
C_e external CO_2 concentration,
C_r assumed as "regulatory" CO_2 concentration,
1.32 originates from calculation of boundary layer resistance for CO_2.

The r_{leaf} was assumed to be equal to the resistance measured by porometer, to stomatal resistance.

4. Material and methods

Investigations on stomatal resistance of maize were carried out at the research area of the Pannon Agricultural University of Keszthely, Hungary, in the growing seasons of 1990–1996. Although we had different aims in different years, the subject of the study was the same: investigation of maize diffusive resistance behavior in field conditions. In the time of measurements *Pioneer hybrids* served as test plants which have a short growing season. Two water supply levels were used:

- maize grown at non limited water supply in lysimeter growing chambers,
- control plants with natural rainfall only.

The surface area of the chambers of Thornthwaite type compensation evapotranspirometers was 4 m^2, and the depth of them was 1 m. We filled the chambers with Ramann type brown forest soil, characteristic soil type in the surroundings of Keszthely. Daily sum of evapotranspiration was given by the change in the volume of soil water in the chamber, by additional water supply (irrigation) through the compensation pot and by precipitation values.

Stomatal resistance was measured with transient type porometers. We used a LI-COR 60 version between 1990–1992, and later on an improved model of Delta T Manufacturers, an AP4 type porometer was applied. We constructed daily course of stomatal resistances by using hourly values. In general, the number of repetitions was 3 to 5. In the beginnig of the growing seasons (May–June) both abaxial and adaxial leaf sides were sampled. Later on the lower epidermis was applied for resistance determinations. Place of stomatal resistance samples depended on the purpose of observation: at determination of stomatal resistance variability within a leaf we separated three leaf sections of each blade, at vertical profile observations the bottom — or top — third line of leaves served as sites of measurements. More details on methodology can also be found in the *Result* section.

Plant parameters as plant height, leaf area index, phenological phases and meteorological observation were also made. (The Agrometeorological Station is located on the same place where field trial was conducted.)

6. Results and discussion

In spite of constant 13.3% difference in pore numbers between two leaf sides of maize — 52 and 68 pieces mm^{-2} on upper and lower epidermises, respectively, — measured divergence in stomatal resistance between two leaf surfaces was not the same during the whole growing season. In the beginning of measurements, size of change in resistance between two leaf sides was much higher than the constant distinction of pore numbers would admit. Independently on investigated years in the series between 1992–94, during May and June the stomatal resistance measured on the upper epidermis of plants grown in lysimeters was 28,3% higher than that resistance of the lower leaf side. The resistance variability within canopy with non limited water supply was about 10% higher than resistance change determined in control plant stands (39%). A likely reason of measured decrease in stomatal resistance of lower epidermis can be attributed to special environmental conditions caused by the canopy structure. In May and June the maize stand is "opened" letting a better radiation penetration into the plant stand and serving more light for pore opening of lower epidermis than after the plant canopy closure. Lower epidermises are known to be more sensitive to light than the upper ones (*Burrows* and *Milthrope*, 1976). After canopy closure, because of mutual shading of leaves, light intensity close to lower epidermis decreases and causes a moderate increase in the stomatal resistance compared to resistance values of the lower epidermis of opened canopies. Independently of water supply level, a linear relationship was determined in maize stomatal resistances between two leaf sides of three investigated years during the early '90-es (*Fig. 1*). This result substitutes earlier knowledge about amphystomatous maize resistance behavior in the very beginning of the growing seasons: before canopy closure both leaf surfaces must be sampled and taken into account when average resistance is calculated.

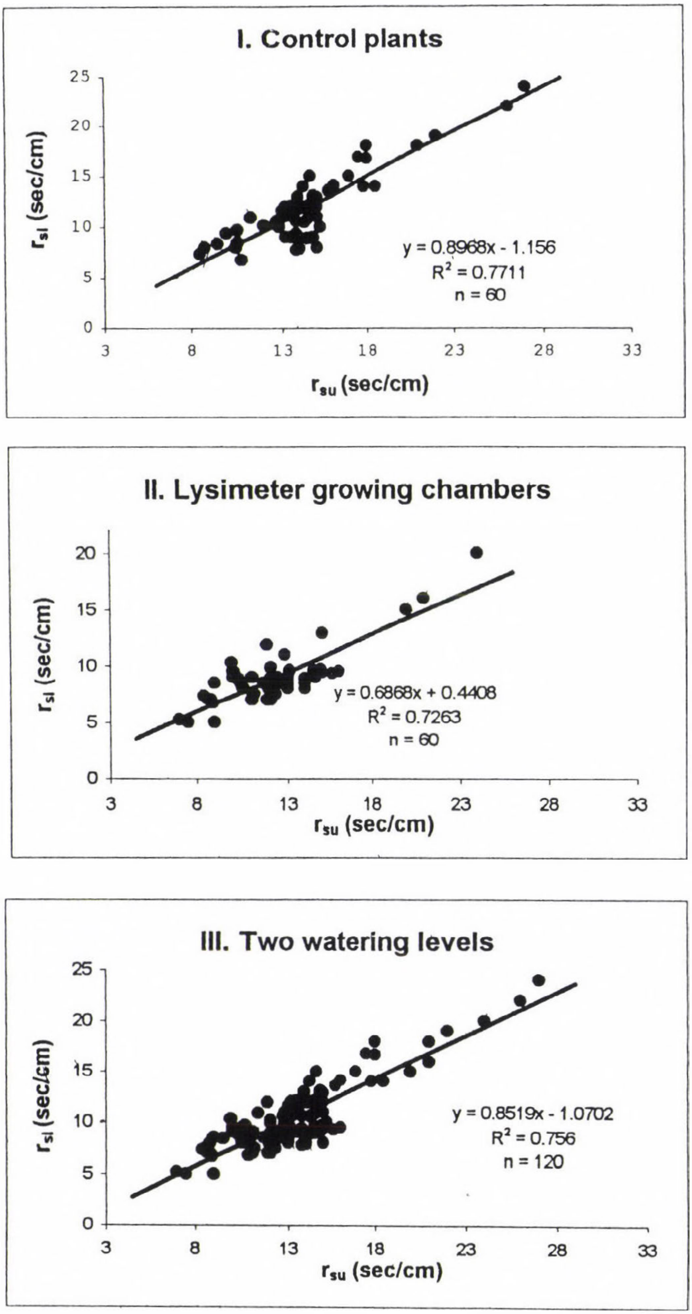

Fig. 1. Relationship of stomatal resistances measured on the upper r_{su} and lower r_{sl} epidermises.

6.1 *Distribution of stomatal resistance within maize plant (Where and how to measure "average" stomatal resistance in the field?)*

Investigation on error at taking stomatal resistance samples was made on six days between 22 July–1 August 1996. We adopted a traditional procedure in stomatal resistance measurements when sample leaves were well insulated, approximately same aged (the youngest) located on top third of the plant height. The mean stomatal resistance for half an hour time period together with statistical parameters of six selected days in the end of July 1996 are presented in *Table 2*. Among sample days there were 4 cloudless and two fully overcast days. Daily number of repetitions (*n*) depended on time necessity of measurements: we repeated observations until the half an hour sample time has finished. On cloudless conditions there were more samples because transit time is shorter than under overcast weather conditions. Plants were grown in lysimeters to decrease the influence of changing water supply on stomatal resistance values. To neglect the influence of altering radiation on pore movements, daily sample times were chosen close to each other, approximately at the same sun angles.

Table 2. Errors in stomatal resistance measurements when samples are taken "accidentally"

Name of measurements Day/Month/Year Sample time (hours)	r_s (sec/cm)	SD*	VC** (%)	No. of sample plants***
Cloudless days				
24/07/1996 10.00–10.30	2.88	1.635	56.64	44
25/07/1996 10.00–10.30	2.61	0.983	37.71	42
31/07/1996 9.40–10.10	3.05	1.096	36.00	45
1/08/1996 11.00–11.30	2.65	0.995	37.55	35
Overcast days				
26/07/1996 10.30–11.00	12.17	9.112	74.84	38
30/07/1996 10.30–11.00	9.97	6.952	69.70	36

SD* : Standard Deviation
VC**: Variation Coefficient
*** : one resistance value per sample plant

Although on completely clear days there was no significant difference in average resistance during the end of July, statistical parameters as SD and VC were not acceptable, mainly during overcast conditions (VC: 69.7–74.84%). These results drew our attention to look for a better place to take resistance samples, to the importance of directed sample taking.

With the better knowledge about stomatal resistance distribution, the likely place of average value can be approximated more precisely and with less energy investments than earlier.

In the first step the sample leaves were chosen accidentally after tasseling, when maize reached its final height. As this method did not produce any valuable result — because of high resistance deviations —, later on the experimental leaves were separated into two categories: for totally sunlit and for completely shaded leaves. This was important, because the influence of radiation seemed to have a more vigorous effect on stomatal resistance than that of the leaf age, that is equivalent to its position on plant level. Fully sunlit approximately same aged (and oriented) leaves are mainly in the top third of plant height. On three to five sample days yearly in July–August of 1992–1996, 10–10 blades were measured around midday (11.00 -15.00 LMT) to neglect the effect of changing radiation on pore movements. The number of sampled days has changed from year to year (finally we had results about 120 leaves). One blade were separated into 6 parts, 3–3 on the right and on the left side from the main rib. Stomatal resistances in 3 to 5 repetitions were registered for each section. Measured leaf section was signed earlier, approximately site of border lines was drawn where significant difference in stomatal resistance had occurred. Finally we had left 3 leaf sections only (360 resistance data) with altered stomatal resistances, because on the right and on the left sides from the rib the resistances differed only casually. Although absolute values of stomatal resistances changed from day to day, their distribution in percentage of whole leaf's mean showed the same tendency: lowest stomatal resistances were measured in the middle of the leaves. The average values of this leaf part were at about 40–45% less, than means of the total leaf area. Reasonable, but always less than 20% increase in resistance was determined on the bottom third of leaf, closest to the stem. The highest resistances can be found on the top of blades, where change in leaf average exceeded 30–35%. A likely reason of this latest increase might have been associated with "self-shading" of maize leaf sections because of their special inclination. (Variation Coefficients were 22, 14 and 31% on the bottom, in the middle and on the top of blades, respectively.)

Completely shaded leaves are positioned on the lower third of plant height close to the soil surface. During our investigation period significant difference in resistance distribution between different blade sections was not measured because of the high deviations of samples, but, like a tendency, a moderate increase in resistances from the stem to the top of blades was registered. Stomatal resistance distribution inside a single shaded leaf was more balanced than resistance distribution of sunny blades, but the variability in resistances between differently oriented (aged) leaves exceeded the variance determined among sunny ones.

After drawing the stomatal resistance distribution of differently positioned leaves, likely site of "average" stomatal resistance — inside a sunny leaf — can be found close to the two border lines dividing the total leaf area into 3 parts. At completely shaded leaves the lower half of the nearest blade third seemed to be the best place for mean resistance measurements. The vertical profile of stomatal resistance of a completely developed maize plant was also drawn (*Fig. 2a*). Each level contains the mean resistance of one leaf. The highest leaf resistances with largest standard deviations occurred in the bottom third of plant height close to soil surface, where shaded leaves are located. The place of the least resistances with a moderately increased standard deviation can be found around the cobs in the middle of plant height. On top level the stomatal resistance showed a reasonable increase compared to the resistance of cob leaves, but this expansion never reached the resistances closest to the soil surface. The vertical profile of resistances and mainly its deviation explain the earlier selection of researchers: top third of height is the place of well-insolated, sunny leaves where the repetition of measurements still gives "acceptable" result with low deviations. But when the purpose of determination is average leaf- (plant-) or mainly crop resistance, a more precise approach should be adopted.

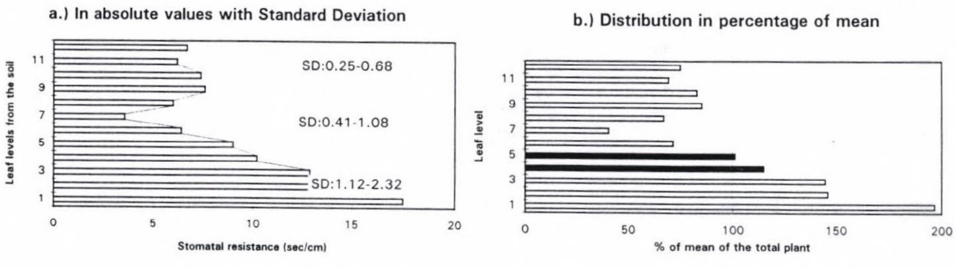

Fig. 2. Vertical profiles of stomatal resistances in maize.

Stomatal resistance of the 2nd or 3rd leaf levels just below the cob seem to be the nearest to the whole plant's average (*Fig. 2b*).

6.2 Verification of the assumption of "average" stomatal resistance

Hourly change in stomatal resistances was simulated under ten soil water potential conditions from -0.1 to –14.0 bars on 25 July 1995 *(Fig. 3)* by using a modified model of Goudriaan. Modification was done by *Chen* (1984), and as a result of this simplification the program was applicable on PC as well. In the same time, in the root zone of lysimeters and control plots –0.28 and -4.3 bars soil water potentials were measured, respectively. During our selected sample day the weather conditions were the best for stomatal resistance measurements, since the sky was completely cloudless and there was no wind.

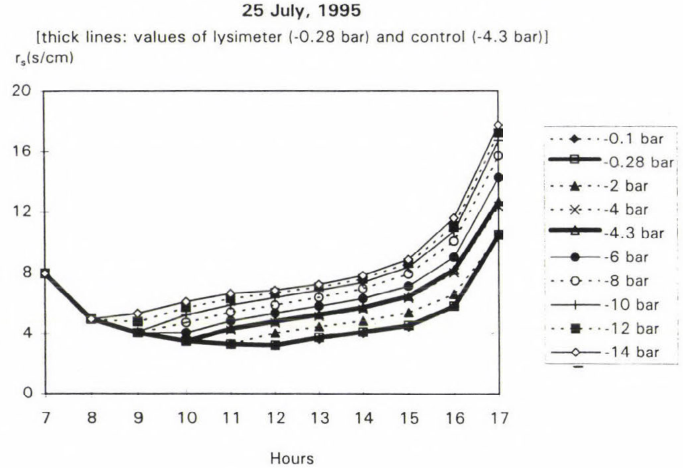

Fig. 3. Daily change in simulated resistances (25 July 1995).

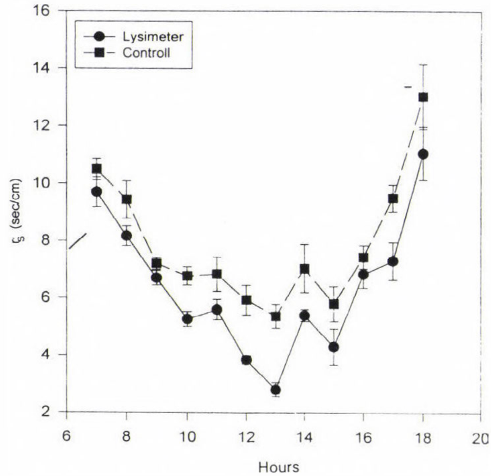

Fig. 4. Daily change in measured stomatal resistances (25 July 1995).

Daily change in measured stomatal resistance of two water supply levels differed significantly *(Fig. 4)*. Highest alteration in hourly resistance values appeared around solar noon. Moderate increase in SD was registered at the beginning and at the end of the measurement period, at low sun angles. Average stomatal resistance of maize plants grown in lysimeters was 21.1% less than the daily mean of control treatments. Change in daily mean of measured and simulated stomatal resistances differed on higher extent, than the averages of two water supply levels (*Fig. 5*). Independently on water supply, in most cases measured resistances can be found below the 1:1 lines: the simulation procedure produces higher resistances than that of the measured ones at high insolation. Simulation of maize stomatal resistance in lysimeters gave better agreement than in case of the control plots. Differences in daily mean stomatal resistances were 8.1% and 12.0% at non limited water supply and the control treatments respectively. Although the values of simulated and measured stomatal resistances were very close to each other for 25 July 1995, at undisturbed radiation and calm weather, then under variable radiation conditions, when the sky is cloudy, the differences in hourly values of simulated and measured stomatal resistance increase, sometimes exceeding 30–40%. However these results are not of universal validity yet, and need further investigations.

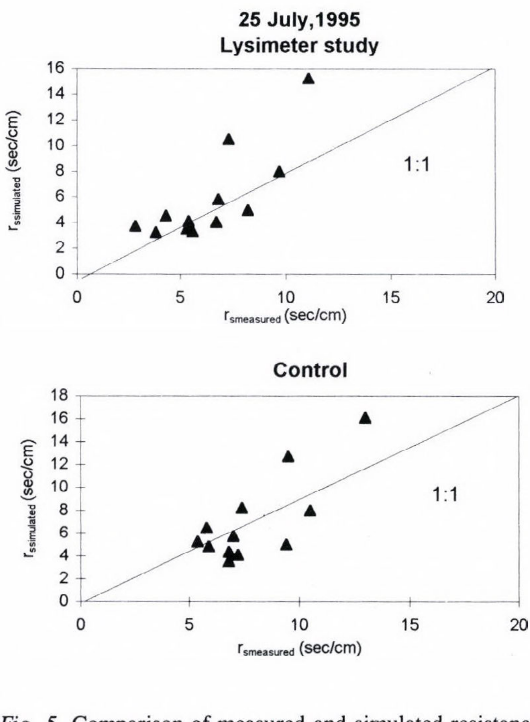

Fig. 5. Comparison of measured and simulated resistances.

References

Burrows, F.J. and *Milthrope, F.L.*, 1976: Stomatal conductance in the control of gas exchange. In *Water Deficit and Plant Growth* (ed.: *T.T. Kozlowski*). Vol. IV. Academic Press, New York-San Francisco-London, pp. 103-147.

Chen, J., 1984: Mathematical analysis and simulation of crop micrometeorology. *Ph.D. Thesis*. The Netherlands.

Goudriaan, J., 1977: *Crop Micrometeorology: A Simulation Study*. Simulation monographs. Pudoc, Wageningen.

Kozlowsky, T.T., 1976: Water deficits and plant growth. In *Soil Water Measurement, Plant Responses, and Breeding for Drought Resistance*. Vol. IV. Academic Press, New York–San Francisco–London.

Monteith, J.L., 1965: Evaporation and environment. *Symp. Soc. Exp. Biol. XIX.*, 205-234.

Pearcy, R.W., *Ehleringer, J.*, *Mooney, H.A.* and *Rundel, P.W.*, 1991: *Plant Physiological Ecology*. Chapman and Hall, London-New York-Tokyo-Melbourne-Madras.

Stiger, C.J., *Goudriaan, J.*, *Bottemanne, F.A.*, *Birnie, J.*, *Lengkeek, J.G.* and *Simba, L.*, 1977: Experimental evaluation of a crop microclimate simulation model for Indian corn (Zea mays). *Agric. Met. 18*, 163-186.

Van Laar, H.H., *Kremer, D.* and *De Vit, C.T.*, 1977: Maize. In *Crop Photosynthesis: Methods and Compilation of Data Obtained with a Mobile Field Equipment*. Agric. Res. Rep. 865. Pudoc, Wageningen, pp. 12-22.

IDŐJÁRÁS

Quarterly Journal of the Hungarian Meteorological Service
Vol. 101, No. 4, October–December 1997, pp. 289–305

Constant pressure balloon–satellite observing system simulation experiments

R. Randriamampianina[1] and **E. P. Borisenkov**[2]

[1]*Hungarian Meteorological Service, Satellite Research Laboratory, P.O. Box 39, H-1675 Budapest, Hungary; E-mail: roger@met.hu*

[2]*Main Geophysical Observatory, 7 Karbisev str., 94018 St. Petersburg, Russia*

(Manuscript received 11 October 1997; final form 14 November 1997)

Abstract—In order to get meteorological information from remote areas, satellite observations are the only available tools. Since satellite observations produce *indirectly* measured data, *a priori* information is required for the retrieval. We studied the possibilities of using an observation system that contains constant pressure balloons together with satellites (CPB-satellite complexes). Mathematical model has been worked out for the estimation of the coverage level of CPBs in the studied area (the Northern Hemisphere). A good distribution of CPBs was found and recommendations have been given about an optimal CPB launching system which can guarantee the necessary level of coverage. Methodological principles and algorithms have been worked out for the synchronization of CPB-satellite complex data in space and time, including: (a) the study of the vertical extrapolation method of the meteorological values; (b) the study of the dynamical initialization method; (c) the development of a new method for the assimilation of the retrieved discretely measured data; (d) the statistical analysis of the horizontal field structure of the meteorological values. Numerical experiments have been carried out to examine the possibilities of CPB and satellite data assimilation. The possibilities and the accuracy of the 4-dimensional data assimilation based on a Numerical Weather Prediction (NWP) model have been estimated. The simulation experiments showed a weak positive impact of simulated CPB data on forecasts.

Key-words: constant pressure balloon, trajectory calculation, optimization problem, data assimilation, dynamical initialization, optimum interpolation, vertical extrapolation.

1. Introduction

For the further development of the World Weather Watch it is necessary to improve the quality of observations over oceans and territories that are difficult to access. However further development of the conventional observation systems for these territories does not seem to be promising.

Therefore satellites and other, non-conventional observation systems (balloons, ships etc.) perform special interest. Remote sensing is a powerful tool to get information from far off territories. In order to retrieve remotely sensed geophysical parameters (e.g. vertical temperature profiles) initial or first guess values (i.e. initial or first guess temperature profiles in the mentioned case) are needed (*Smith et al.*, 1985; *Eyre*, 1989). In practice, climatological data, statistical regression or output of an NWP model are used as initial profiles. This kind of information can be supplemented with data observed by CPBs — e.g. tetrons — equipped with temperature sensors that transmit information through satellites (*Borisenkov et al.*, 1982; *Lally et al.,* 1967). Since the CPB data are independent from the satellite data, a new task has to be solved, namely the simultaneous assimilation of synchronous (conventional) and asynchronous (non-conventional, like balloons, satellites etc.) information.

Since the realization of experiments using a CPB-satellite complex is a very expensive and complicated task, the method of numerical simulation of the CPB observations on the basis of a hydrodynamical model of the atmosphere was chosen as the main research method.

The next section of the paper will introduce a short review of the use of balloons in meteorology. The third section will describe the experiments about the trajectory analysis and the spatial-temporal coverage by CPBs over the Northern Hemisphere. The observation system simulation experiments will be described in section 4 while section 5 contains the results and conclusions.

2. The application of CPBs in meteorology and related research

Balloons have been used as scientific tools from the end of the 18th century. Since the tracing of balloons as well as the transmission of the information from the balloons to the Earth became possible using satellites, the utilization of balloons for meteorological purposes gained more perspective. In particular, the idea of a global observation system containing a large number of balloons together with other systems came up.

In *Borisenkov et al.* (1982), the use of meteorological balloons in different international meteorological and environmental projects is well described. Thus, the meteorological balloons were used in several investigations for the following purposes:

- To study the atmosphere over the Pacific Ocean;
- For the vertical sounding of the atmosphere: projects EOLE, TWERLE and GHOST (*Lally et al.,* 1967);
- To study the atmospheric circulation in the Tropics: project TWERLE;
- To study the dynamics of monsoon: project TWERLE and exp. Balsamine.
- For trajectory forecast and hindcast over Australia (*Mills et al.,* 1994);
- To derive tracer plume trajectories during ETEX (European Tracer Experiment) (*Koffi et al.,* 1997).

3. Design of the numerical experiments with simulated CPBs

In the present study two numerical experiments were accomplished to examine the behavior of the CPBs in the atmosphere:

Exp. 1. The calculation of the trajectories of the balloons.

Exp. 2. The study of the most appropriate balloon-launching method for getting the optimum coverage of the territory.

When studying the behavior of the balloons, we used the GARP (Global Atmospheric Research Program) data which include:

- data of geopotential, temperature, wind speed components and dew-point temperature for levels 1000, 850, 700, 500, 300 and 100 hPa;
- relative humidity data for levels 1000, 850, 700, 500 and 300 hPa.

The data were presented on a regular grid in the spherical coordinate system. We carried out the transformation of the data into the Cartesian coordinate system using polar stereographic projection on latitude 60°.

3.1 Analysis of the trajectories of CPBs

The goal was to study the path of the balloons to decide whether they can fly separately from each other or just follow the jet stream.

The trajectories of 17 balloons, theoretically launched from different latitudes and longitudes of the Northern Hemisphere were calculated according to Eq. (1) (*Fig. 1*).

$$X_{\eta}^{t+\Delta T} = X_{\eta}^{t} + m_{\varphi\eta} \cdot \Delta t \cdot U_{\eta}^{t}, \qquad (1)$$

where $X_{\eta}^{\alpha} = \left(x_{\eta}^{\alpha}, y_{\eta}^{\alpha}\right)$ is the coordinate vector of the balloon in the Cartesian co-ordinate system; $U_{\eta}^{\alpha} = \left(u_{\eta}^{\alpha}, v_{\eta}^{\alpha}\right)$ is the wind speed; $\alpha = t$ or $t + \Delta t$ is the index of time; $m_{\varphi\eta} = 1.866/(1 + \sin \varphi_{\eta})$ is the mapping parameter; η is the index of CPB.

For this experiment we used the data received from the GARP project for the summer and winter period of 1979. For the summer period the starting day was 5 June 1979, for winter — 1 January 1979. In both cases data of 20 days were used.

According to the results (Fig. 1), one complete turn of CPBs around the globe required about 20 days. The balloons did not cross the Equator and the tendency of displacement to higher or lower latitudes was not significant. A good agreement between the behavior of the balloons and the zonality of the atmosphere was obtained during the flight in summer and in winter as well — accumulation of balloons could not be observed.

Since CPBs can fly over territories that are difficult to access they can assure a good coverage of the Northern Hemisphere. Therefore the next experiment was to examine the spatial-temporal distribution of the CPBs over the Northern Hemisphere.

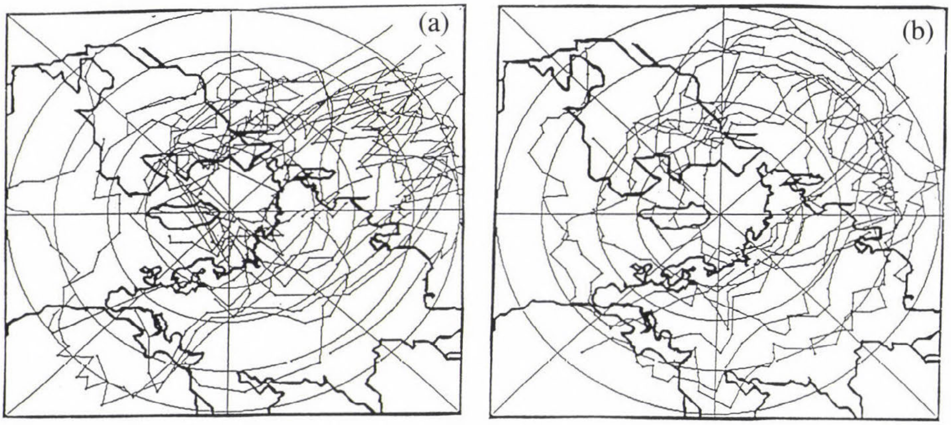

Fig. 1. The trajectory of CPBs (*a*) in winter, (*b*) in summer.

3.2. Study of the spatial-temporal coverage of the investigated area

The main task of the observation systems is to detect the state and the evolution of the meteorological elements and the physical parameters of the surface. Perturbations of the meteorological fields are caused by atmospheric motion systems characterized by their intensity, geometrical size and life time. On this basis atmospheric motion systems are often identified with and called as perturbations. The spatial-temporal characteristics of the observation system determine the accuracy of measurements of different scale perturbations. The "ideal" observation system should be able to detect the whole cycle of any perturbation from the moment of its arising till the end of its existence. In practice, this criterion applies only to synoptic scale or larger perturbations ($L \geq 5000$ km).

One of the methods to establish the minimum required density of a radiosounding network is to determine the influence radius of synoptic-scale atmospheric perturbations. According to the calculations (*Reshetov,* 1973) the required density of sounding on stratospheric levels (200–10 hPa) should be around 500–1000 km, which corresponds to the demands of the World Meteorological Organization. In the GARP project the recommended resolution of a CPB system on 200 hPa level was 500 km (*Bengtsson,* 1975). In this case the minimum number of balloons would be around 220–320 when investigating the Northern Hemisphere — excluding any accumulation of balloons resulted by either flux convergence, diffusion or vertical movement.

The estimation of the degree of accumulation of the balloons on 200 hPa level in the Southern Hemisphere was one of the goals of the EOLE project in 1971–72 (*Sitbon,* 1975). According to the experiments the distribution of the balloons over the Southern Hemisphere was almost uniform.

The aim of our study was to decide whether it is possible using a smaller amount of periodically launched CPBs to reach the *minimum required* coverage level of the Northern Hemisphere.

Since the number of balloons as well as the launching points were not identified at the beginning of this rather complicated investigation, several series of experiments were accomplished. Therefore, a certain number of CPBs were launched 12 hourly:

(1) 140 balloons in 2 days (*Fig. 2* and *Fig. 3a*);

(2) 40 balloons in 3 days (*Fig. 2* and *Fig. 3b*).

The space resolution of sounding (P) was determined based on the distances between the balloons. In case of 140 balloons the mean space resolution of sounding for the "model area" (due to the stereographic projection, it is smaller than the Northern Hemisphere area) was 480 km.

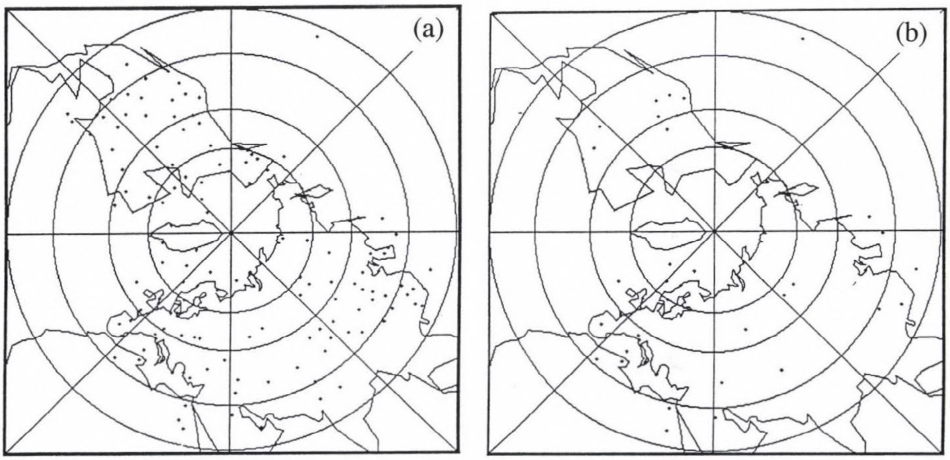

Fig. 2. Launching positions of CPBs; (*a*) 140 CPBs, (*b*) 40 CPBs.

By increasing the number of CPBs we could decrease the frequency of their launch. The period between the launches at the beginning can be chosen freely — 6 hours, 12 hours or 24 hours etc. —, but as soon as the coverage of the studied area reaches the necessary level for the concrete task, we can increase the interval between the launches up to 24 hours, 36 hours etc. According to our calculations, for example, in case of launching 140 CPBs at the beginning, we can increase the intervals between their launches on the third day (mean P about 480 km), while starting only with 40 CPBs (mean P about 640 km, after the second day) we need at least 4–6 days to obtain the same amount of information as in the first case.

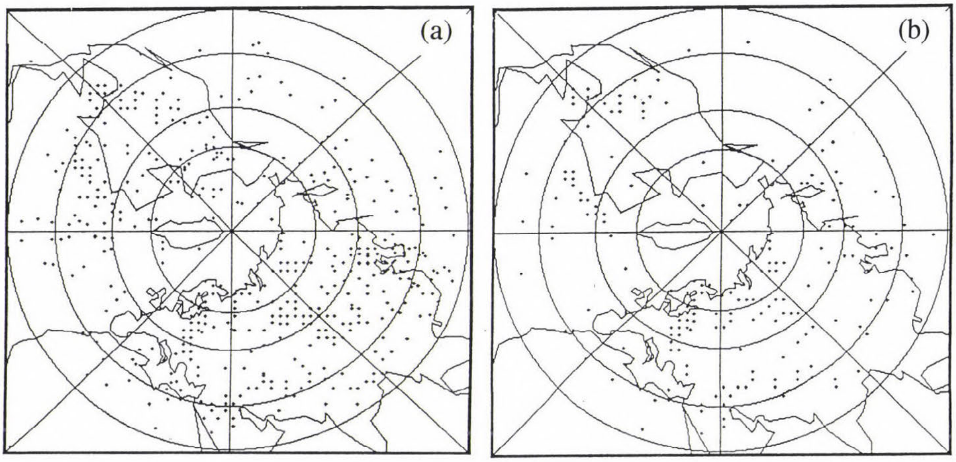

Fig. 3. Position of CPBs after the second day of launching using (*a*) 140 pieces, (*b*) 40 pieces.

The optimum number of CPBs strongly depends on the objective of the study. For example, when studying the synoptic situation in the atmosphere some dozens of CPBs could turn out to be enough and the frequency of their launching could be decreased in 3–4 days after starting. Such results are comparable with the results of other investigations (*Borisenkov et al.,* 1982). However, for applying CPB data as a *first guess* to assimilate satellite data (e.g. TOVS) one should use a greater number of CPBs (about 100), having about a 4-day *preliminary launching*[1] from places well separated from each other.

Based on the results discussed above, the realization of a CPB-satellite observation system which includes CPBs transmitting information through satellites (for example geostationary orbital satellites) seems to be feasible. The offered CPB system could be realized by using light weight balloons and could prove to be considerably cheaper than using the same amount of radiosondes. Some economic calculations are published in *Borisenkov et al.* (1982). The presented method, applied and realized on computer permits to model any kind of CPB-launching strategy based on real data.

[1] By preliminary launching we mean the period during which we reach the necessary coverage and after which we can decrease the frequency of launching.

4. Observing System Simulation Experiments (OSSE)

All simulation experiments have been performed by applying the adiabatic version of the hemispheric prognostic NWP model developed at the Russian Hydrometeorological Centre (Moscow, Russia) with the contribution of the Russian State Hydrometeorological Institute (St. Petersburg, Russia). This model is based on the dynamical equations of the atmosphere in quasi-static approximation (*Berkovitch,* 1982; *Berkovitch et al.,* 1982, 1985; *Kritchak*, 1981).

In order to perform the four-dimensional analysis, we used the geopotential, temperature, humidity and horizontal wind vector data taken from TEMP and SATEM information. We could not use TOVS radiance data because even if we had been able to get them we would have had a computer memory problem. Since we could not use real data measured by CPBs the calculation of balloon paths as well as the calculation of data that could have been measured by CPBs were carried out.

To analyze the impact of CPBs on the observing system the following numerical experiments (A, B, C) for four-dimensional data assimilation have been accomplished using the *continuous* data assimilation system (*Fig. 4*):

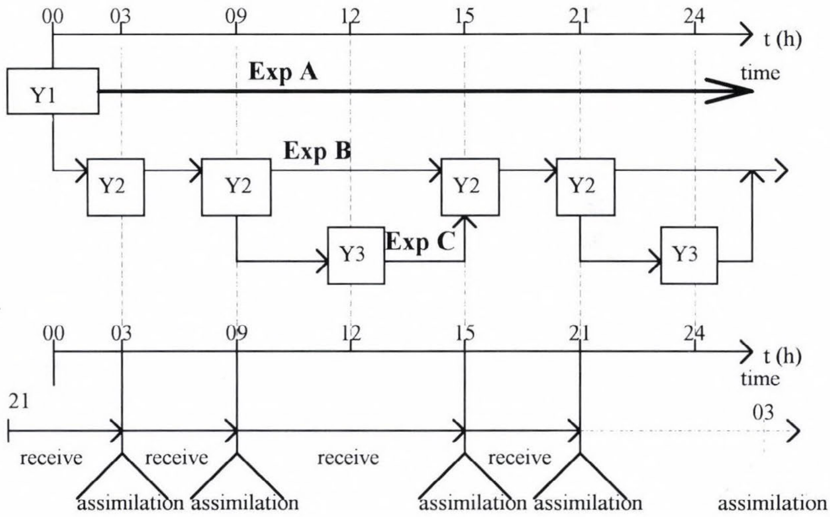

Fig. 4. Time steps of the data assimilation scheme.

Exp. A: 24 hour forecast.

Exp. B: Assimilation of SATEM and balloon data:

B1: run with SATEM data only;

B2: run with SATEM and balloon data (supposing "on level" measurements);

B3: run with SATEM and balloon data (supposing vertical profile measurements).

Exp. C: Assimilation of all available (SATEM, TEMP, balloon) data:

C1: run with TEMP, SATEM and balloon data (supposing "on level" measurements);

C2: run with TEMP, SATEM and balloon data (supposing vertical profile measurements);

C3: run with TEMP and SATEM data only.

This way of carrying out the experiments allowed us to estimate the impact of the balloon data on the assimilated fields.

4.1 Data assimilation schemes

Usually the data assimilation cycle is performed every 6 hours: 00, 06, 12 and 18 UTC. In the scheme applied in these analyses (see Fig. 4) there is a time displacement between the assimilation of the remotely sensed data (Y2) and the conventional ones (Y3). Such a structure allows to separate the asynchronous data from the synchronous ones (TEMP) and makes it possible to evaluate the impact of balloons on the forecast. Hereafter we give detailed description of **the important steps** in the different blocks of the assimilation scheme.

Y1. (Fig. 4): Initial data processing includes data interpolation to the grid.

Y2. (*Figs*. 4, 5): Assimilation of asynchronous (SATEM and CPB) data.

Step 1. The model uses Arakawa C grids, but it is more convenient to use uniform grids when assimilating the data.

Step 2. Simulation of the data of CPB measurements.

The simulated observation errors were calculated as a sum of two types of errors: random error and systematic error. If we assume that we can measure two variables, the air temperature and the geopotential height, we can model them as:

$$T_\eta^M = (\beta_T)_\eta + (E_T)_\eta + (E_T)_s \tag{2}$$

$$H_\eta^M = (\beta_H)_\eta + (E_H)_\eta + (E_H)_s \tag{3}$$

where β denotes the background values; H and T are the indices of the background values of the geopotential height or temperature; M is the index of the simulated values; s is the index of the systematic error; η is the index of CBP.

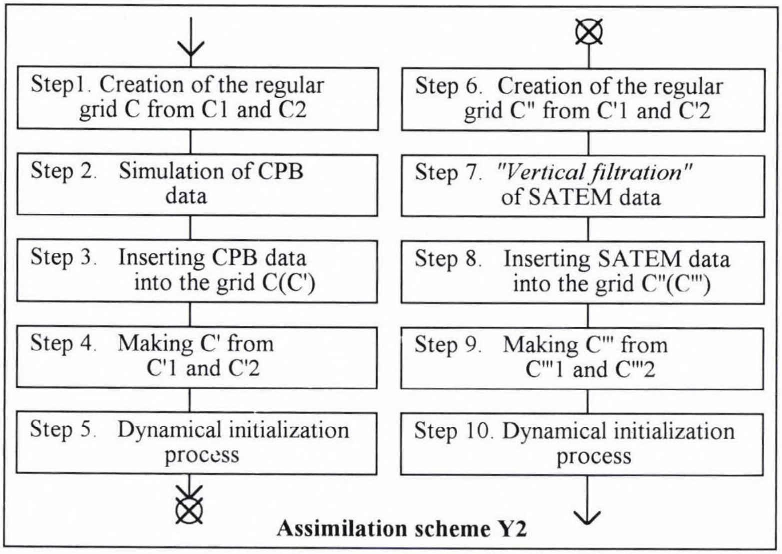

Fig. 5. Assimilation scheme for asynchronous data.

The generator of the random error is a random variable ξ for which:

$$-1 \le \xi(\sigma) \le 1, \tag{4}$$

where σ is an arbitrary random event. For an arbitrary error E_η:

$$-E_x \le E_\eta \le E_x, \tag{5}$$

where $E_\eta = \xi_\eta(E_x)$; E_x is the maximum possible error; x is a meteorological variable.

In case of vertical profile observations from balloons we have to simulate the "measured" profiles as well taking into account the profile of the systematic error of the geopotential height and the temperature. The following scheme was used to extrapolate data from the level of measurement in order to establish the profile in case of "on level" observation with balloons:

$$\gamma_\eta = \frac{1}{4}\sum_{i}^{i+1}\sum_{j}^{j+1}\gamma_{i,j}, \tag{6}$$

$$\gamma_{i,j} = \frac{\beta^T_{i,j,k+1} - \beta^T_{i,j,k}}{\beta^H_{i,j,k+1} - \beta^H_{i,j,k}}, \tag{7}$$

$$H^M_{\eta,k+1} = H^M_{\eta,k} + \frac{\overline{\beta^T_{\eta,k}}}{\gamma_\eta}\left[\left(\frac{P_{k+1}}{P_k}\right)^{\frac{-R\gamma_\eta}{g_0}} - 1\right] \quad \text{if} \quad \gamma \neq 0, \tag{8}$$

$$H^M_{\eta,k+1} = H^M_{\eta,k} + \frac{\overline{R\beta^T_{\eta,k}}}{g_0} \ln\left(\frac{P_{k+1}}{P_k}\right) \qquad \text{if} \quad \gamma = 0, \tag{9}$$

where R is the gas constant for dry air; *i, j* are indices of the nearest grid point; k is the index of the model level; g_0 is the average value of the force of gravity on sea-level; $\overline{\beta^T}$ is the average grid background value.

$$\overline{\beta^T_{\eta,k}} = \frac{1}{4} \sum_{i}^{i+1} \sum_{j}^{j+1} (\beta_T)_{i,j}. \tag{10}$$

$T^M_{\eta,k+1}$ is calculated as below:

$$T^M_{\eta,k+1} = T^M_{\eta,k} + \gamma_\eta \left(H^M_{\eta,k+1} - H^M_{\eta,k}\right). \tag{11}$$

Step 5. For the dynamical assimilation the forward-backward method has been chosen.

Step 7. For the assimilation of satellite data we used the method described in *Lorenc* (1986). The assimilation of the relative humidity data was performed according to *Filiberti et al.* (1994) for levels 300, 500 and 700 hPa. For the other levels (where we did not have data of precipitable water amount) we used the equation given by *Tarakanova* in *Czelnai et al.* (1976) for the calculation of relative humidity. The assimilation of geopotential data was carried out by using the following algorithm:

(1) Geopotential thickness between 1000 hPa and P_k:

$$\Delta H_{g,k} = -(H_{1000} - H_k). \tag{12}$$

(2) Mean virtual temperature between P_0 and P_k:

$$T_{m,k} = \frac{g_0 \Delta H_{g,k}}{R \ln \frac{P_0}{P_k}}. \tag{13}$$

(3) Control: $$D_k = \Delta H_{g,k} - \Delta H_{s,k}.$$

Profiles were not taken into account if $P_0 < 1000$ hPa;
For $D_k > 500$ m: $$\hat{T}_{m,k} = T_{m,k}.$$

(4) $$\hat{T}_{m,i} = T_{m,i} + C K^T (K C K^T + E)^{-1} \cdot \left(\Delta H_{s,i} - \Delta H_{g,i}\right). \tag{14}$$

(5) $$\Delta \hat{H}_k = \frac{R \hat{T}_{m,k}}{g_0} \cdot \ln \frac{P_0}{P_k}, \tag{15}$$

(6) $$H_k = \Delta \hat{H}_k + H_{1000,g}, \tag{16}$$

where k is the index of the level, i is the index of the profile, g is the index of the background value, C is the error covariance matrix of T_m, s is the index indicating the satellite data, E is the observation error covariance matrix and K is a diagonal matrix, consisting of the elements $\frac{R}{g_0} \cdot \ln \frac{P_0}{P_k}$, $k = 1, 2 \ldots$

Y2' (*Figs*. 4, *6*): Corrected version of the scheme Y2.

When applying scheme Y2, data were put on the grid in such a way that the nearest point on the grid had been identified for each data and its value had been given directly to that point. Simulation results demonstrated, however, that such an approach disturbs the horizontal structure of the meteorological fields (Fig. 8a). Therefore we decided to apply scheme Y2' (Fig. 6). In Y2' optimum interpolation (*Gandin et al.*, 1976) was included for assigning the data to the grid points.

Y3. (*Figs*. 4, *7*): This scheme was used when including the TEMP data into the analysis.

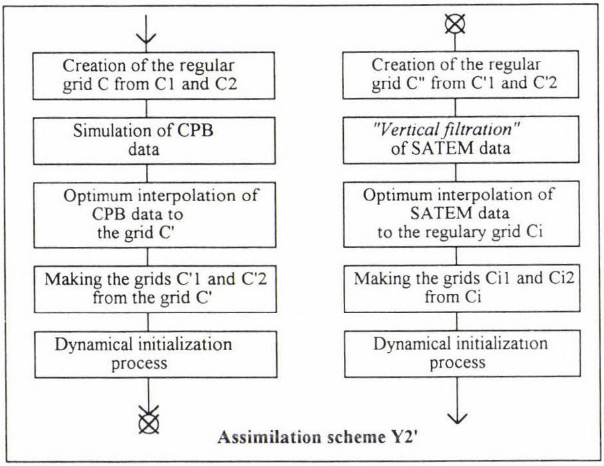

Fig. 6. Corrected assimilation scheme for asynchronous data.

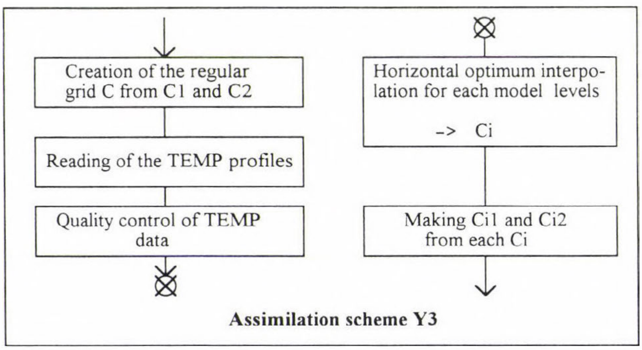

Fig. 7. Assimilation scheme for conventional data.

5. Results and conclusions

Evaluating briefly each of the methods that have been used, we can conclude the following:

(1) The dynamical initialization method has been tested on the basis of specially created noise[2]. The evaluation has been carried out using the results of the assimilation after four cycles of pseudo-forecast forward and

[2] The noises were created by adding non-realistic random values to the geopotential fields (see Eqs. (2) and (3) without systematic part of the errors) at randomly chosen points of the Northern Hemisphere.

backward (*Fig. 8a, 8b*). We can note a positive change of the structure of meteorological fields.

(2) The bias of the optimum interpolation of TEMP data (geopotential field for the 500 hPa level, at 12.00 UTC on 24.09.1993) into the grids is presented on *Fig. 9*. The results show that inside the observation area the error of optimum interpolation is small and it increases towards the edges.

(3) The improvement of the relative humidity field retrieved using the quantity of precipitable water (SATEM) is presented on *Fig. 10* for the 700 hPa level. Comparing the maps we can note that after the assimilation the relative humidity field changed in a positive way. We can observe analogous changes in the case of the retrieval of the geopotential using Step 7 of the block Y2 (*Fig. 11*) in the assimilation scheme.

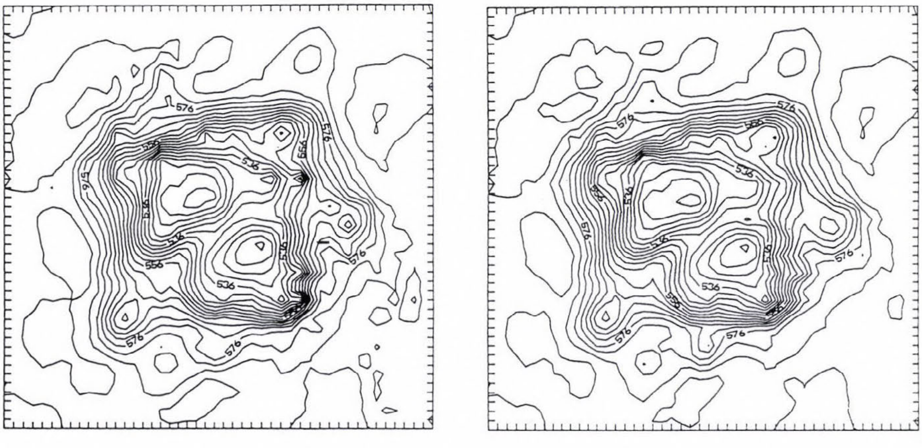

Fig. 8. 500 hPa geopotential field: before (*a*) and after (*b*) dynamical initialization (Y2); (03.00 UTC 24.09.1993; unit is 10 m).

From the assimilation results of the CPB-satellite complex the following conclusions can be made using quantitative evaluation (see Fig. 12 and Fig. 13):

(1) The impact of SATEM data on the forecast (exp. B1) is slightly positive. This result does not contradict the conclusions of earlier studies (*Eyre*, 1989; *Eyre et al.*, 1989; *Filiberti et al.*, 1994; *Riley et al.*, 1995) according to which it is difficult to show the positive impact of the satellite data in the Northern Hemisphere. On the other hand, using variational technique, a bigger impact of SATEM data in the Northern Hemisphere was found with the French forecasting system (ARPEGE) (*Randriamampianina et al.*, 1997). The accuracy of the analysis is outstanding for the 1000 hPa level field.

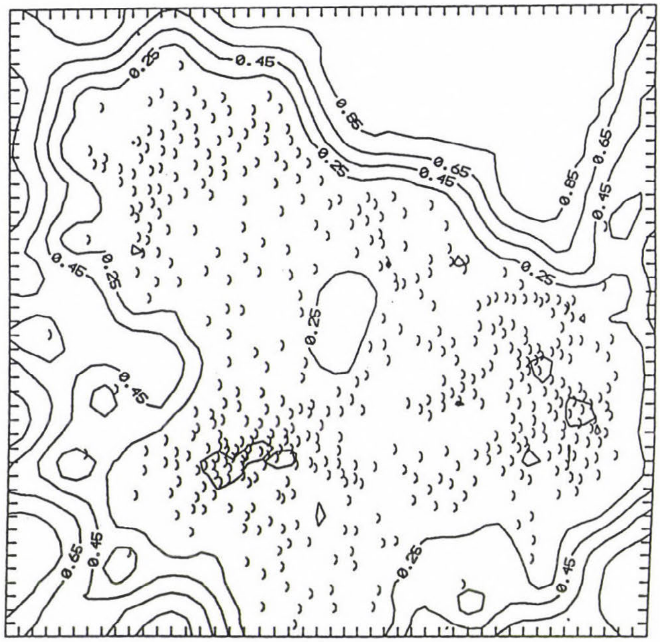

Fig. 9. Relative error of OI of TEMP data to the grid (geopotential field for the 500 hPa level at 12.00 UTC 24.09.1993).

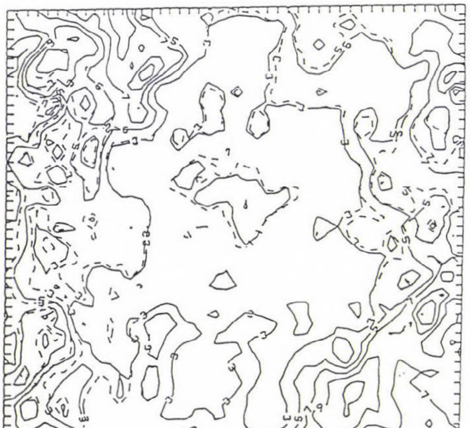

Fig. 10. 700 hPa relative humidity field before (dashed) and after (solid) the assimilation; (21.00 UTC 24.09.1993; unit is g/kg).

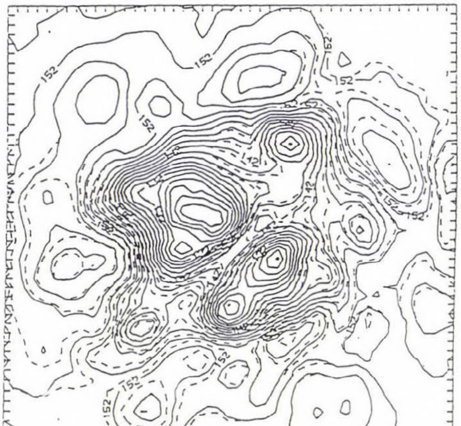

Fig. 11. 850 hPa geopotential field before (dashed) and after (solid) the assimilation; (21.00 UTC 24.09.1993; unit is 10 m).

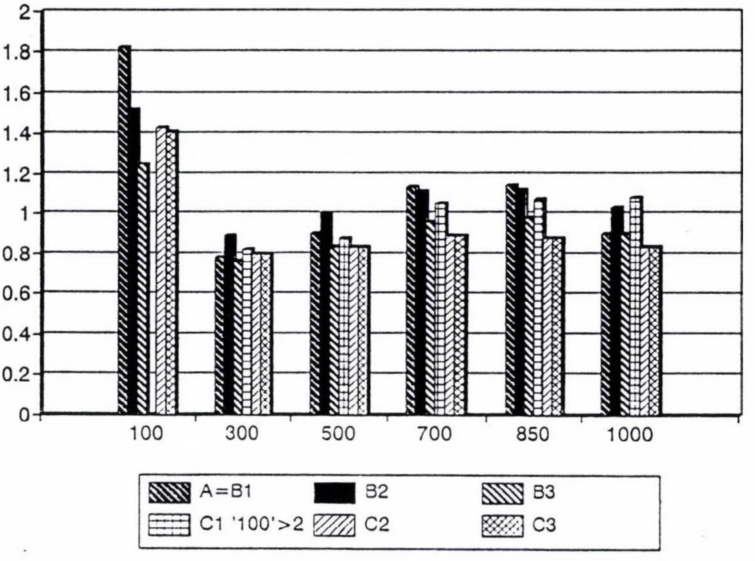

Fig. 12. Root mean square error of geopotential after 24 hour assimilation on the 100, 300, 500, 700, 850 and 1000 hPa levels.

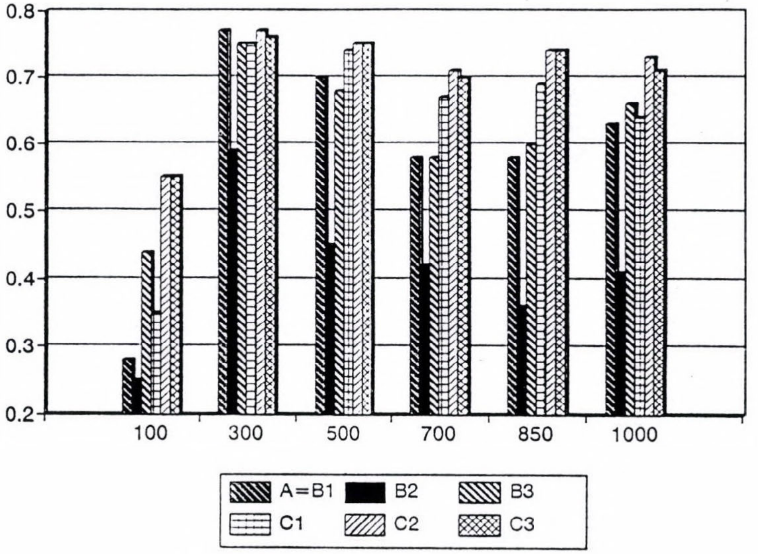

Fig. 13. Correlation between NMC and our analyses after 24 hour assimilation on the 100, 300, 500, 700, 850 and 1000 hPa levels.

(2) The chosen vertical extrapolation method is very poor. As a consequence, analysis B2 became even worse than B1, with the exception of the 300 hPa level. Therefore, it is necessary to improve the extrapolation method.

(3) All results of the assimilated fields improved in case of the assumption that CPBs can make measurements of vertical profiles of meteorological elements — see exp. B3 (the correlation for the 100 hPa level, for example, was around 0.44, while it was 0.25–0.28 in the other cases).

(4) In case of experiments of the third group (C) we could reach a considerable improvement by adding TEMP data to the assimilation. However the problem of data extrapolation still exists in this case of assimilating all available data. We also received the best results when we used vertical CPB measurements (C2).

Therefore, applying the CPB-satellite measurement complex with vertical CPB measurements one can improve the quality of the analyses of asynchronous data. In the case of "on level" CPB measurements however, the improvement of vertical data extrapolation is very important as well.

The perspectives of efficiently using a 4D assimilation based on balloon-satellite observation system seem to be the following:

(1) The model-assimilator used in the present study is a quite simple one — a hemispheric adiabatic model with 300 km resolution. It would be necessary to add non-adiabatic factors to get more reliable results.

(2) When starting this study we intended to use more observation types in the assimilation. However, we faced a lot of problems related to the available data and computer memory limit; so only the TEMP and SATEM data were used. It is necessary to mention here that we were given data only for a two-day period (24 09 1993–25 09 1993). In order to be able to draw more valid conclusions when studying the impact of CPB data on the analysis of synchronous and asynchronous observations, a longer experimental period is required.

(3) In *Borisenkov et al.* (1982) CPBs were assumed to be suitable for performing vertical profile measurements. It would be interesting to consider the possibility of using CPBs that could carry out vertical profile measurements based on LIDAR or RADAR principles.

(4) It would be interesting to perform the same experiments treating the satellite–CPB system as an autonomous source of all measured data in 4D assimilation.

Acknowledgements—Partial support for this work has been provided by Hungarian Scientific Joint Foundation F015963 and T014933. The authors wish to thank *B. D. Panin, T. Práger, G. Major, J. Pailleux, Yu. A. Pichugin, O. M. Pokrovski* and *Zs. Ruzsbatzky* for helpful discussions.

References

Bengtsson, L., 1975: 4-dimensional assimilation of meteorological observation. *GARP Publication series*, No. 15. 75 p.

Berkovitch, L.V. and *Tkachev, Yu.V.*, 1982: A non-adiabatic hemispherical model of atmosphere for forecast of meteorological elements up to some days (in Russian). *Trudy GMC USSR*, edition 242.

Berkovitch, L.V and *Tkachev, Yu.V.*, 1985: The evolution of the hemispherical atmospheric model (in Russian). *Trudy GMC USSR*, edition 277.

Berkovitch, L.V., 1982: A six levels scheme of forecast based on completes equations for a large territory (in Russian). *Trudy GMC USSR*, edition 100.

Borisenkov, E.P., Alter-Zalik, Yu.G. and *Kuznitsov, A.D.*, 1982: *Atmospheric Sounding with Meteorological Balloon* (in Russian). Gidrometeoizdat, Leningrad, 176 p.

Czelnai, R, Gandin, L.S. and *Zachariew, W.I.*, 1976: *Statistical Structure of Meteorological Fields.* Hungarian Meteorological Service.

Eyre, J.R., 1989: Inversion of cloudy satellite sounding radiances by nonlinear optimal estimation. I: Theory and simulation for TOVS. *Quart. J. Roy. Meteorol. Soc. 115*, 1001-1026.

Eyre, J.R. and *Lorenc, A.C.*, 1989: Direct use of satellite sounding radiances in numerical weather prediction. *Meteorological Magazine 118.*

Filiberti, M.A., Eymard, L. and *Urban, B.*, 1994: Assimilation of satellite precipitable water in a meteorological forecast model. *Quart. J. Roy. Meteorol. Soc. 122*, 486-506.

Gandin L.S. and *Kagan, R.L*, 1976: *Statistical Interpolation Methods of Meteorological Fields.* Gidrometeoizdat, Leningrad, 356 p.

Koffi, E., Nodop, K. and *Bénech, B.*, 1997: Constant volume balloon model used to derive tracer plume trajectories (ETEX experiment first release). *ETEX symposium on long-range transport, model verification and emergency response*, 13-16 May 1997, Vienna Austria.

Koffi, E., Nodop, K. and *Bénech, B.*, 1997: Constant volume balloon model used to derive tracer plume trajectories (ETEX experiment second release). *ETEX symposium on long-range transport, model verification and emergency response*, 13-16 May 1997, Vienna Austria.

Kritchak, S.O., 1981: A non-adiabatic model of atmosphere based on primitive equations to forecast the meteorological elements above Europe (in Russian). *Met. and Hydr.*, edition 7.

Mills, G.A., Downey, W.K. and *Whitby, F.*, 1994: Trajectory calculations in support of meteorological planning and forecasting for two transcontinental balloon flights. *Aust. Met. Mag. 43*, 29-39.

Lally, V.E. and *Rickel, A.B.*, 1967: Project GHOST. *Science*, 1967 June, 60-65.

Lorenc, A.C., 1986: *Technical Proceedings of the Second International TOVS Study Conference.* 18-22 Feb 1985, Igls, Austria, pp. 224-253.

Randriamampianina, R., Pailleux, J., Thépaut, J.-N. and *Moll, P.*, 1997: The impact of the satellite TOVS data in 3D variational analysis at Météo France. *Technical Proceedings of the ninth International TOVS Study Conference*, 20-26 Feb 1997, Igls, Austria.

Riley, P., Steinle, P., Hart, T. and *Kelly, G.*, 1995: The impact of 1DVAR TOVS retrievals compared to NESDIS retrievals on 5 day global forecasts. *Technical proceedings of the eighth international TOVS study conference*, Queenstown, New Zealand.

Reshetov, V.D., 1973: *Variability of Meteorological Elements* (in Russian). Gidrometeoizdat, Leningrad.

Sitbon, P., 1975: Platform location and data collection by satellite systems. The EOLE experiment. *IEEE Trans. Geosci. Electron. 13*, No. 1, 2-17.

Smith, W.L., Woolf, H.M., Hayden, C.M. and *Schreiner, A.J.*, 1985: *Technical Proceedings of the Second International TOVS Study Conference*, 18-22 Feb 1985, Igls, Austria, pp. 224-253.

BOOK REVIEW

Ernő Mészáros: **Atmospheric Chemistry** (in Hungarian). *Issued by:* Veszprémi Egyetemi Kiadó. 57 figures and 22 tables, 167 pages.

The principal goal of the book is to discuss the chemical processes and related phase transitions occurring in the Earth's atmosphere. They are in close connection with the biogeochemical cycle of elements and the consequences of anthropogenic activity. The book contains 8 *Chapters* and 4 *Annexes*.

Chapter 1 summarizes the basic characteristics of the atmospheric radiation transfer, photochemical and thermal reactions as well as the formation of free radicals in the atmosphere. In *Chapter 2* the chemistry of upper atmosphere is described including the structure of the ionosphere (E, F and D layers). *Chapter 3* is dedicated to the ozone problem in three sub-chapters: Homogeneous chemistry of the stratosphere; Heterogenous processes in the stratosphere (with special attention to the formation of ozone hole); Tropospheric ozone. In *Chapter 4* reader is provided with the explanation of gas-phase reactions of carbonaceous components. Reduced and oxidized sulfur compounds are discussed in *Chapter 5*, including the emission, chemical transformation and deposition of these species. *Chapter 6* describes the characteristics, dynamics and chemical composition of aerosol particles. Effects of particles on climate control are also discussed in this chapter. The role of water in the control of chemical processes, including cloud and precipitation formation, deposition processes of trace components as well as chemical composition of cloud and precipitating water is presented in *Chapter 7.* Basic atmospheric transport models and their applications are introduced in the last chapter. It is also emphasized here that modeling can only be a powerful tool in the case if it is applied together with high quality measurements. More than 100 references are cited for the eight chapters.

The textbook is proposed to read first of all for students studying chemistry, meteorology, environmental engineering and environmental sciences, however, it will be useful for scientist who are interested in a young science between meteorology and chemistry, in close connection with the problems of environmental protection. Most recent and widely published atmospheric issues like stratospheric ozone hole formation or tropospheric ozone formation in pollutant air are explained in details in the book.

László Bozó

NEWS

Second Conference on Forest and Climate (SCFC) Sopron, Hungary 4–6 June 1997

Hungarian meteorologists, foresters, biologists and ecologists held a common meeting for the second time in order to discuss the interrelation of the forest and climate as well as the impact of global warming first of all on the ecosystem and on the modification of the radiation-, heat- and water-budget of the forest. The responsible experts, as participants of the First Conference on Forest and Climate (FCFC) in Noszvaj (Hungary) from 1–3 June 1994, agreed to announce that such common scientific meeting should be organized in the future, as well. They thought that every three years so much new results would gather in our country in the research of the interrelation system of forest and climate that these could be discussed in a common meeting by the interested specialists.

In the spirit of the above mentioned thoughts the SCFC was held in Sopron, Hotel "Siesta" located among the beautiful "Lővérek" (pine forests), 4-6 June 1997.

The unusually successful, effective and very instructive scientific conference was organized by the Meteorological Department of Kossuth Lajos University of Debrecen and the Department of Science of Knowledge for the Arable Site of the Forestry University of Sopron with the support of the Debrecen Team of the Hungarian Meteorological Society, the National Forestry Assembly and the Meteorological Working Group of the Territorial Commission in Debrecen of the Hungarian Academy of Sciences.

The papers delivered at the conference were focused on discussing the newest results reached in the field of the following three main subjects:

- new results in Hungary in the topic of a possible climate change (global warming),
- development possibilities of the forestry climate classifying methods,
- interrelations between the forestal ecosystem and the atmospheric processes near the ground.

These topics show that the forestry climatology (whose founder in our country was *Károly Botvay*, professor of the University of Sopron) covers a wide range of relations between forestal and environmental factors, implies environmental changes on micro- and macro-scales, as well as local and regional environmental problems. When having defined the subjects of the conference, the role of meteorological transfer processes in the formation of micro-climate of the forest stand, as a new investigational branch, was stressed.

As it is known, these processes are based on a self-adjusting system of dynamical processes of the radiation-, heat- and water-balance in the forestal ecosystems (stands) and between the forest and atmospheric layers near the ground, as well.

Since the microclimate of the forest is controlled by processes of energy balance, when the call for papers was issued the conference organizers emphasized that the processes of energy transformation of the forest stand should be studied, known and understood with an increasing intensity. Namely, the expected and also under way modifications of forest climate, which are produced by the joint effect of the global environmental changes (warming, acid rain, ozone layer depletion, concentration increase of air pollutants, modification of global circulation systems, decrease of diversity of fauna and flora species, consequences of global social and economical changes, etc.) and the local forest management (cultivation, deforestation, afforestation) can be modelled and forecasted only if we know these processes.

Nearly hundred participants listened to 43 papers about the mentioned topics. Besides papers treating general relationships, information was given about numerous investigational results based on in situ measurements in some forests (Sopron Hills, Síkfőkút, Mátra, Park Forest of Pilis, Zala Hills), while directing an outstanding attention to oaks, beeches, spruces and mixed forest stands in lowlands. Similarly to the FCFC, at this meeting several papers were also concerned with the role of noxious insects depending on climate. The relation between the forest management and climate change, the damage done by sleet, mapping of environmental evaluation as well as energetic utilization of the forestry waste were also mentioned.

Meteorological "output" of the conference were a survey of regional consequences of global climate change in terms of scenarios, the establishment of possibilities and limitations of genetical and migration conditions of the forest adaptation, and the assessment of the rate of spatial and temporal variations of trends and extremes in the time series of precipitation and temperature.

More than ten presentations dealt with the changes of radiation-, heat- and water-budget components and temperature, precipitation and soil moisture conditions within the forest stand, moreover with nitrogen budget and the exchange conditions of trace gases in the forestal ecosystems. Furthermore, the audience could get information about a few new measuring and calculating techniques, which have been applied by Hungarian scientists to discover the microclimatic and ecological system of the forest. Some papers discussed the causes of the forest degradation and outlined the tasks of forestry for saving and meliorating the forest stands.

As it was already emphasized by the speakers and contributors at the FCFC the hygienic state of our forests has been gradually deteriorating in which the drought, occurring with greater frequency and greater intensity in the last two decades than earlier, has played a significant role. The more frequently observed, prolonged and considerable lack of precipitation has caused that the forestal ecosystems is becoming feebler and consequently there is a degradation of individuals of some species. This process is accelerated by the acid rain water and the multiplication of pathogens due to the more extreme weather phenomena. It seemed to be proved that as a consequence of the anthropogenic activities the forestal ecosystem became more sensitive and more vulnerable. This tendency is certainly strengthened by global changes (among others global warming) and it may be assumed that these variations are faster than the acclimatization ability of biocenosises of forests — as it was established by the participants of the conference.

The investigational achievements in topics discussed at the SCFC not only increase the scientific knowledge but can contribute to the scientific foundation of a more modern forest management, to the planning of the afforestation, considering environmental conditions of the next century, and to the professional foundation of the expansion of our forested areas (in the future decades a new afforestation in an area of about one million hectare is planned in Hungary, which will increase the forested area of our country by one-third part of the present extension). The participants of the SCFC also expressed their desire that the newest forestry investigational results should be considered and utilized when the Hungarian Parliament will codify a new forest law in the future. For this reason the conference formulated proposals, and a working group was deputed to compile their final version. The organizers are intending to publish the papers presented at the conference, including the proposals as well.

On the first afternoon of the conference the participants, professionally guided by *Péter Víg* first assistant, could study the radiation-, heat- and water-balance measuring station of the University of Sopron on the site in the forests of Sopron Hills region. It was an outstanding program of the conference, when a statue of *Prof. Károly Botvay* was inaugurated in the Botanical Garden of the University of Sopron.

The successful organization of the SCFC may be owed to *Dr. Károly Tar* university lecturer, the leader of the Meteorological Department (Kossuth Lajos University of Debrecen) and *Dr. Péter Víg* first assistant (University of Sopron) as well as their co-workers who performed really cautious, tiring and altruistic work. On behalf of the conference participants I would like to express my congratulations and thanks to the above mentioned colleagues for the excellent organizing of this meeting which was very useful and enjoyable for all participants.

Emánuel Antal

The 1997 EUMETSAT Meteorological Satellite Data Users' Conference Brussels, Belgium 29 September–3 October 1997

The 1997 EUMETSAT Meteorological Satellite Data Users' Conference was held in Brussels from 27 September to 3 October. Earlier the Meteosat and NOAA Users' conferences were organized separately in every two years, but from the previous year they are joined into one common conference. In this year the conference was organized and sponsored by the European Organization for Exploitation of Meteorological Satellites (EUMETSAT) and the Belgian Royal Meteorological Institute.

The conference began with the opening remarks by the Minister of Sciences of Belgium, the head of the Belgian Royal Meteorological Institute and *Dr. Tillmann Mohr*, the director of EUMETSAT.

The conference gave good opportunity for the users of data of the meteorological satellites to exchange experiences. New methods, applications and algorithms were presented mainly for Meteosat and NOAA data, but there were also presentations on GOES satellite data and application of microwave instrument SSM/I of DMSP American satellite. We obtained useful information on other geostationary satellites as well, like the Russian GOMS, INSAT of India and technical characteristics of the Chinese meteorological satellite to be lunched soon.

The presentations were separated into five sessions: Operational applications, Data processing, Pre-processing for products, Derivation of geophysical parameters and Current and future satellite systems. Two additional sessions were organized, one on Calibration and the other on Satellite Application Facility (SAF) groups. In addition to the oral sessions, a poster session, including software presentations, was also held; this, concerning the principal importance of the visualization of satellite imagery, proved to be highly useful and efficient. The posters were hanged in the foyer of the auditorium during the whole week, and all poster authors held a 3-minutes verbal presentation as well.

The short-wave spectral bands of Meteosat and NOAA satellites do not have in-flight calibration. The 1. and 2. channels of NOAA/AVHRR instrument have pre-launch calibration but the visible cannel of Meteosat does not have any. A special session was held on methods of the indirect after-launch calibration and the cross-calibration of the different satellites.

A large number of presentations reported on cloud detection and cloud classification. For NOAA satellites these methods are mostly threshold methods like the APOLLO (for the region of the Alps) and the SCANDIA (developed for Sweden), but methods based on statistical investigations were also shown. For the region of the Alps a cloud coverage statistics for a five year period was presented. The SCANDIA method applies more thresholds, it is not only for cloud detection but also for cloud classification. For Meteosat images a method called MET'clock was presented for cloud detection and cloud top height retrieving.

Several talks discussed the methods for detection of meso-scale convective systems and estimation of the expected rainfall.

Other papers presented methods for identification of clouds giving a large amount of precipitation and for rainfall estimation. For the mid-latitudes these methods apply simultaneously SSM/I and NOAA/AVHRR data.

The operational cloud motion wind vectors are among the most important products retrieved from Meteosat data. Many presentations were held on this topic, on the accuracy of the vectors and on further developments.

Other papers presented methods for the application of satellite information in vegetation monitoring and crop yield estimation. Investigations were shown on fire detection mostly for the tropics but also for Spain.

In the last session the plans for the main further developments were presented. The expected launch time of the Meteosat Second Generation (MSG) is October 2000. The SEVIRI, the imagery system of the MSG will be ready in February 1999. EUMETSAT plans to launch two new own quasi-polar orbiters called METOP. The new version of American NOAA satellites will be launched in 1998 working with 6 or 7 channels.

In the Education Program of EUMETSAT an interactive program package is elaborated, some parts of that is already working on the Internet in field of satellite meteorology and numerical prediction (http://eumetsat.meteo.fr).

Dr. Anikó Rimóczi-Paál presented a paper titled 'Mapping of Radiation Balance Components for Hungary Using Meteosat Data' in the session Derivation of Geophysical Parameters. *Dr. Mária Putsay* presented a poster titled 'Atmospheric correction of NOAA/AVHRR visible and near-IR channels in Hungary'. Both presentations drew a great interest, and some scientists asked for reprints.

The presented papers will be published in the conference proceedings.

The next conference in this field will be organized in Paris, in May 1998 by METEO-France.

Mária Putsay
Anikó Rimóczi-Paál

ATMOSPHERIC ENVIRONMENT

an international journal

To promote the distribution of Atmospheric Environment *Időjárás* publishes regularly the contents of this important journal. For further information the interested reader is asked to contact *Prof. P. Brimblecombe*, School for Environmental Sciences, University of East Anglia, Norwich NR4 7TJ, U.K.; E-mail: atmos_env@uea.ac.uk

Volume 31 Number 14 1997

The Lower Fraser Valley oxidants/Pacific '93 field study

Volume 31 Number 15 1997

Volume 31 Number 16 1997

Special Issue on the Great Dunn Fell Clad Experiment 1993, Eurotrac sub-project Ground-based Cloud Experiment (GCE)

Volume 31 Number 17 1997

Short Communication

IDŐJÁRÁS

VOLUME 101 * 1997

BUDAPEST, HUNGARY

AUTHOR INDEX

TABLE OF CONTENTS
I. Papers

II. Book review

III. News

Contents of journal Atmospheric Environment, 1997

IV. SUBJECT INDEX

The asterisk denotes book review or news

A

NOTES TO CONTRIBUTORS

The purpose of *Időjárás* is to publish papers in the field of theoretical and applied meteorology. These may be reports on new results of scientific investigations, critical review articles summarizing current problems in certain subject, or shorter contributions dealing with a specific question. Authors may be of any nationality but papers are published only in English.

Papers will be subjected to constructive criticism by unidentified referees.

* * *

The manuscript should meet the following formal requirements:

Title should contain the title of the paper, the names(s) of the author(s) with indication of the name and address of employment.

The title should be followed by an *abstract* containing the aim, method and conclusions of the scientific investigation. After the abstract, the *key-words* of the content of the paper must be given.

Three copies of the manuscript, typed with double space, should be sent to the Editor-in-Chief: *P.O. Box 39, H-1675 Budapest,* Hungary.

References: The text citation should contain the name(s) of the author(s) in Italic letter or underlined and the year of publication. In case of one author: *Miller* (1989), or if the name of the author cannot be fitted into the text: *(Miller,* 1989); in the case of two authors: *Gamov* and *Cleveland* (1973); if there are more than two authors: *Smith et al.* (1990). When referring to several papers published in the same year by the same author, the year of publication should be followed by letters a,b etc. At the end of the paper the list of references should be arranged alphabetically. For an article: the name(s) of author(s) in Italics or underlined, year, title of article, name of journal, volume number (the latter two in Italics or underlined) and pages. E.g. *Nathan, K. K.,* 1986: A note on the relationship between photosynthetically active radiation and cloud amount. *Időjárás 90,* 10-13. For a book: the name(s) of author(s), year, title of the book (all in Italics or underlined with except of the year), publisher and place of publication. E.g. *Junge, C. E.,* 1963: *Air Chemistry and Radioactivity.* Academic Press, New York and London.

Figures should be prepared entirely in black India ink upon transparent paper or copied by a good quality copier. A series of figures should be attached to each copy of the manuscript. The legends of figures should be given on a separate sheet. Photographs of good quality may be provided in black and white.

Tables should be marked by Arabic numbers and provided on separate sheets together with relevant captions. In one table the column number is maximum 13 if possible. One column should not contain more than five characters.

Mathematical formulas and *symbols:* non-Latin letters and hand-written marks should be explained by making marginal notes in pencil.

The final text should be submitted both in manuscript form and on *diskette.* Use standard 3.5" or 5.25" DOS formatted diskettes for this purpose. The following word processors are supported: WordPerfect 5.1, WordPerfect for Windows 5.1, Microsoft Word 5.5, Microsoft Word 6.0. In all other cases the preferred text format is ASCII.

* * *

Authors receive 30 *reprints* free of charge. Additional reprints may be ordered at the authors' expense when sending back the proofs to the Editorial Office.

Published by the Hungarian Meteorological Service

Budapest, Hungary

INDEX: 26 361

HU ISSN 0324-6329